

**Illinois Water Resources Center
Annual Technical Report
FY 2009**

Introduction

The Illinois Water Resources Center is located on the University of Illinois Campus in Urbana-Champaign and serves people throughout Illinois. The state spans from the highly urban Chicago metro region in the northeast to rural southern Illinois and touches many of the central US's major water ways including the Great Lakes, the Mississippi and Ohio Rivers.

In 2009, IWRC researchers, with funding from 104B supported two graduate student initiated research projects. Outreach and technology transfer activities included two conferences, publications of a newsletter and web site, and interactions with agencies through the Midwest Technology Assistance Center, the State Water Supply Task Force and many others.

Research Program Introduction

None.

Award No. G09AP00026 Two-Dimensional Modeling of Hydrodynamics and Sediment Transport in St. Clair River

Basic Information

Title:	Award No. G09AP00026 Two-Dimensional Modeling of Hydrodynamics and Sediment Transport in St. Clair River
Project Number:	2008IL198S
Start Date:	1/1/2009
End Date:	6/30/2009
Funding Source:	Supplemental
Congressional District:	
Research Category:	Engineering
Focus Category:	Hydrology, Sediments, Models
Descriptors:	Hydrodynamics, models, sediment transport
Principal Investigators:	, Gary Parker

Publications

There are no publications.

Research Project Report

**Modeling of Hydrodynamics and Sediment Transport in
St. Clair River**

Submitted

To

International Joint Commission (IJC)

International Upper Great Lakes Study (IUGLS)

by

Xiaofeng Liu¹ and Gary Parker²

¹Postdoctoral Research Associate, Ven Te Chow Hydrosystems Laboratory, Department of Civil and Environmental Engineering, University of Illinois at Urbana and Champaign, IL

²Professor, Department of Civil and Environmental Engineering and Department of Geology, University of Illinois at Urbana and Champaign, IL

April, 2009



ILLINOIS
UNIVERSITY OF ILLINOIS AT URBANA-CHAMPAIGN

Table of Content

1. Introduction.....	2
2. Calibrations and Mesh Independence	3
2.1 Calibrations	3
2.1.1 Roughness Calculation for the First Two Bends	4
2.2 Mesh Independence Study	6
3. 3D Numerical Model Verifications	8
4. HydroSed2D Model Applications	10
4.1 Shear Stress Distribution.....	10
4.2 Bathymetry Change Effects	12
4.2.1 Two-dimensional Modeling and Analysis.....	12
4.2.2 One-dimensional Backwater Curve Analysis.....	14
4.2.3 Two-lake Problem and Conveyance Change Analysis.....	17
4.3 Lake Huron Inlet Alignment Effects	19
5. Sediment Transport and Armoring Analysis	21
5.1 Gravel Transport	21
5.2 Sand Transport	27
5.3 Glacial Till Erosion Test and Analysis	30
6. Ice Cover and Ice Jam Effects.....	30
6.1 Flow Redistribution Effect under an Ice Cover.....	30
6.2 Could the record St. Clair River ice jam of 1984 cause significant erosion?.....	31
6. Navigation Effects.....	33
8. Conclusions.....	35
Appendix A	37
References.....	39

1. Introduction

The continuous lowering of Lake Michigan-Huron levels has caused increasing concerns. St. Clair River, which drains Lakes Michigan and Huron to Lake St. Clair-Lake Erie, appears to bear much of the blame. Among many others, Baird & Associates (2005) investigated the possible causes. The three most possible ones appear to be: erosion of the St. Clair River bed, relative change in net basin supply (NBS), and differential glacial rebound. These hypotheses are still under investigation.

Dredging activities for navigation and mining of sand and gravel in the river bed can be dated back to the 1800's. Three major dredging projects in the history of the river can be identified: dredging for the 6.1m navigation channel completed in 1906, the 7.6m (25ft) navigation channel completed in 1937, and the 8.2m (27ft) navigation channel completed in 1962. Dredging and erosion so induced appears to have changed the river conveyance. Sand and gravel mining have also contributed to the change of the river bathymetry.

Changes of the cross section at some critical points (due to e.g. shipwrecks) may also have affected the conveyance. These changes of the cross section are due to human settlement and development. The modification of the cross section may have changed the flow in the river and therefore affected the water level in Lake Michigan and Lake Huron.

The sediment supply into the St. Clair River has changed over time. Shoreline protection and numerous harbor structures in Lake Huron, especially around the area near the St. Clair River outlet, appear to have locally reduced the sediment transport rate. The sediment feed rate at the inlet of the St. Clair River, while probably never large due to the presence of Lake Huron, may have been further reduced by e.g. groins. These factors could have caused erosion of the river bed and therefore change in the conveyance.

In our work, an in-house numerical code, HydroSed2D, will be used. HydroSed2D is a two-dimensional depth-averaged hydrodynamic code with sediment transport (Liu and García, 2008). It is based on the shallow water equations. This code was originally developed by Prof. Alistair Bothwick at University of Oxford, UK. The original code uses a quad-tree grid structure. It has been used in many engineering applications, including scour due to dyke breaching in the Yellow River, China. We have adapted HydroSed2D for unstructured meshes and made it easy to be applied to complicated domains. The Godunov scheme is used to solve the governing equations. The details of the code can be found in Liu (2008).

After a high quality mesh is generated and the HydroSed2D model is carefully calibrated, the model is used to investigate the possible causes of the Lake Huron level dropping, namely the bathymetry change and the Lake Huron inlet alignment. Bathymetry data from year 1971 to 2008 are used. Shear stress distribution in the river is plotted and its implication for sediment transport is analyzed.

Sediment transport and armoring analysis is done by combining the HydroSed2D model and the Microsoft Excel tool Acronym for gravel transport. The shear stresses from the HydroSed2D model and the sediment size distributions from image analysis are used as input for armoring calculation.

Other factors, such as ice cover/ice jam and navigation, are also investigated. Their effects on the river flow and sediment transport are qualitatively analyzed. Rough estimations are made according to measurement in the literature.

2. Calibrations and Mesh Independence

Before any simulations can be carried out, two things need to be done to control the quality of the results: the calibrations and the mesh independence study.

2.1 Calibrations

The roughness is important since it is the parameter which defines the drag force experience by the flow. On the other hand, the shear force on the river bottom by the flow is the driving force of the sediment movement. The purpose of the calibration runs is to adjust the roughness of the river bed. The roughness of the first two bends area is determined by sediment sizes based on the analysis of the under water images. The rest of the river reach is divided into several zones. The division of the reach is shown in Figure 1. The zones for roughness: (a) the whole river (b) the upstream part In each zone, the Manning's n is adjusted to match the simulated water surface elevations with the measurements. The roughness of the river is not constant. It dynamically changes when the river evolves. The man made changes, such as the gravel mining, navigation, dredging, and ship wreckage, affect the roughness to some extend. The response of the river itself, such as the armoring effect, sediment transport, will also change the roughness. These dynamic changes of the flow resistance involve many unknowns and will be too complicated to be modeled. As such, they are not modeled in the present study.

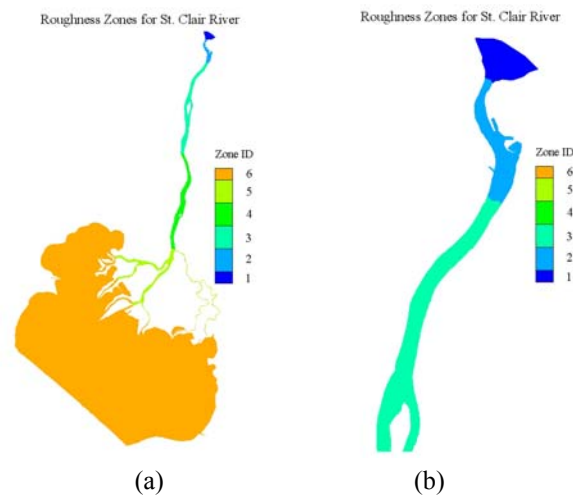


Figure 1. The zones for roughness: (a) the whole river (b) the upstream part

2.1.1 Roughness Calculation for the First Two Bends

The bed shear stress can be made dimensionless as

$$C_f = \frac{\tau_b}{\rho U^2}$$

Where C_f is the dimensionless bed resistance coefficient, the dimensionless Chezy resistance coefficient C_z is related to C_f as

$$C_z = C_f^{-1/2}$$

Keulegan (1938) proposed a formulation for the Chezy coefficient:

$$C_z = C_f^{-1/2} = \frac{1}{\kappa} \ln \left(11 \frac{H}{k_s} \right)$$

where $\kappa = 0.4$ denotes the dimensionless Karman constant and k_s = a roughness height characterizing the bumpiness of the bed.

Manning-Strickler formulation:

$$C_z = C_f^{-1/2} = \alpha_r \left(\frac{H}{k_s} \right)^{1/6}$$

where α_r is a dimensionless constant between 8 and 9. Parker (1991) suggested a value of α_r of 8.1 for gravel-bed streams, which is also used in this research.

Roughness height over a flat bed:

$$k_s = n_k D_{s90}$$

where D_{s90} denotes the surface sediment size such that 90 percent of the surface material is finer, and n_k is a dimensionless number between 1.5 and 3. In this research, the value of n_k is fixed as 2.

The calculation is shown in Table 1.

Table 1. Roughness calculation based on sediment size distribution from images analysis

Image Location	Sediment (use volume)			C_z		Manning n		Strickler Coefficient	
	D_{50} (mm)	D_{90} (mm)	$K_s = n_k * D_{90}$ (mm)	Keulegan (1938)	Manning-Strickler	Keulegan (1938)	Manning-Strickler	Keulegan (1938)	Manning-Strickler
Thalweg 1	27	55	110	16.85	17.18	0.0278	0.0273	35.93	36.63
Thalweg 2	34.4	65.6	131.2	16.42	16.68	0.0286	0.0281	35.02	35.57
Thalweg 3	19	38	76	17.75	18.27	0.0264	0.0257	37.86	38.96
Thalweg 4	26.4	52.5	105	16.96	17.31	0.0276	0.0271	36.18	36.92
					Average:	0.0276	0.0270	36.22	36.98

After some initial trial, three sets of roughness conditions are listed in Table 2 as possible candidates. Three sets of hydraulic condition simulations (see Table 3) were done to determine the roughness (Manning's n) for zone 1, 3, 4, 5, and 6 (roughness for zone 2 comes from image analysis). The three sets of simulations represent the low, medium, and high flow conditions. These typical discharges and stages are chosen from measurement data and special care was taken to make sure the river is at almost steady state during these typical periods.

Table 2. Roughness calibration conditions set
(numbers in red for zone 2 is from sediment size analysis)

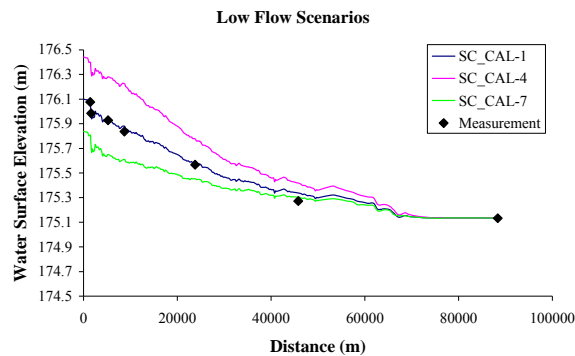
Zone ID	Set 1		Set 2		Set 3	
	Manning's n	Strickler Coefficient	Manning's n	Strickler Coefficient	Manning's n	Strickler Coefficient
1	0.0166	60.2	0.0200	50.0	0.0161	62.0
2	0.0276	36.2	0.0276	36.2	0.0276	36.2
3	0.0250	40.0	0.0333	30.0	0.0167	60.0
4	0.0227	44.0	0.0286	35.0	0.0154	65.0
5	0.0200	50.0	0.0233	43.0	0.0159	63.0
6	0.0213	47.0	0.0278	36.0	0.0192	52.0

Table 3. Three typical hydraulic conditions sets for calibrations

Low Flow Scenario Set 1		Medium Flow Scenario Set 2		High Flow Scenario Set 3	
Discharge (m ³ /s)	Lake St. Clair Level (m)	Discharge (m ³ /s)	Lake St. Clair Level (m)	Discharge (m ³ /s)	Lake St. Clair Level (m)
4645	175.133	5282	174.937	6006	175.513
Date: 4/27/2005		Date: 8/24/2005		Date: 8/1/1998	

Table 4. Nine calibration cases
(combination of roughness sets and hydraulic condition sets)

Case ID	Roughness Condition Set	Hydraulic Condition Set
CAL-1	1	1
CAL-2	1	2
CAL-3	1	3
CAL-4	2	1
CAL-5	2	2
CAL-6	2	3
CAL-7	3	1
CAL-8	3	2
CAL-9	3	3



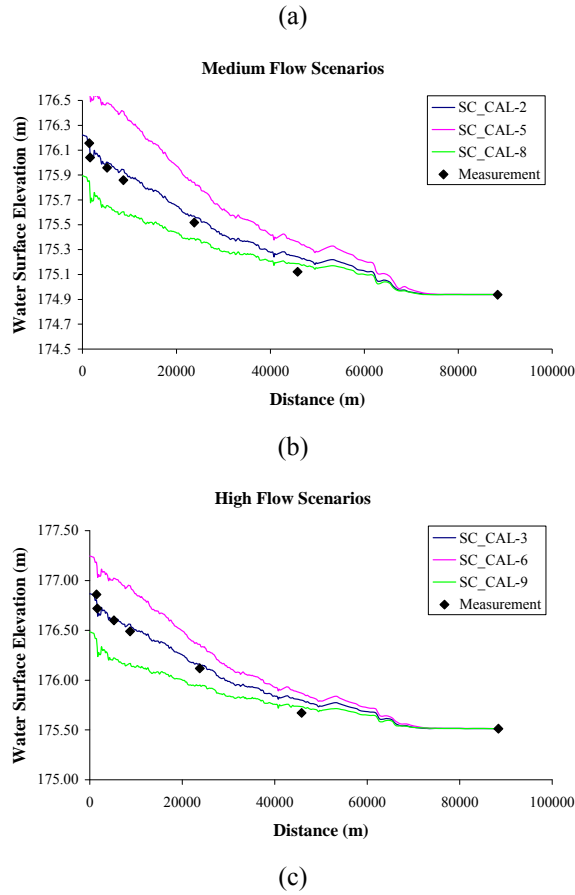


Figure 2. Comparisons between Simulated Results and Measured Stages for Calibration Runs: (a) Low Flow Scenarios (b) Medium Flow Scenarios (c) High Flow Scenarios

2.2 Mesh Independence Study

For a large, as well as complicated, lake-river system of the Lake Huron-St. Clair River-Lake St. Clair, a decent mesh with high quality is important for the creditability of the simulation results. The mesh need to be as fine as possible to capture most of the geometry and bathymetry details. However, it is unrealistic to use a mesh which is too fine since it will dramatically increase the computational time. In order to use a mesh which is neither too fine nor too coarse, a mesh independence study is warranted.

Three different meshes with different refinement are used. The parameters, such as the mesh size, mesh numbers, are listed in Table 5. The mesh for the domain is shown in Figure 3. Special treatment of the meshes is applied to the first two bends. The reason has two folds. First, there are a lot changes around the bends (such as the big scour hole, the tongue features, and historical ship wreckages). This is also the control area for the flow. As shown in the shear stress analysis, the contraction from the Lake Huron to the St. Clair River makes the bottom shear stresses is highest in this area. This implies that sediments in the first two bends have the highest potential of movement. This might lead to the explanation of the tongue features of the sand bars and their

effects in terms of conveyance. Mesh is also refined in the area of the delta in Lake St. Clair. Refined mesh is needed to well represent the narrow navigation channel which controls the water surface elevation throughout the St. Clair River.

Table 5. Three sets of meshes used for mesh independence study

Mesh ID	Cell Numbers	Mesh Size in the First Two Bends (m)	Mesh Size in Other Areas (m)
A	6124	400	800
B	24066	100	200
C	53962	50	200

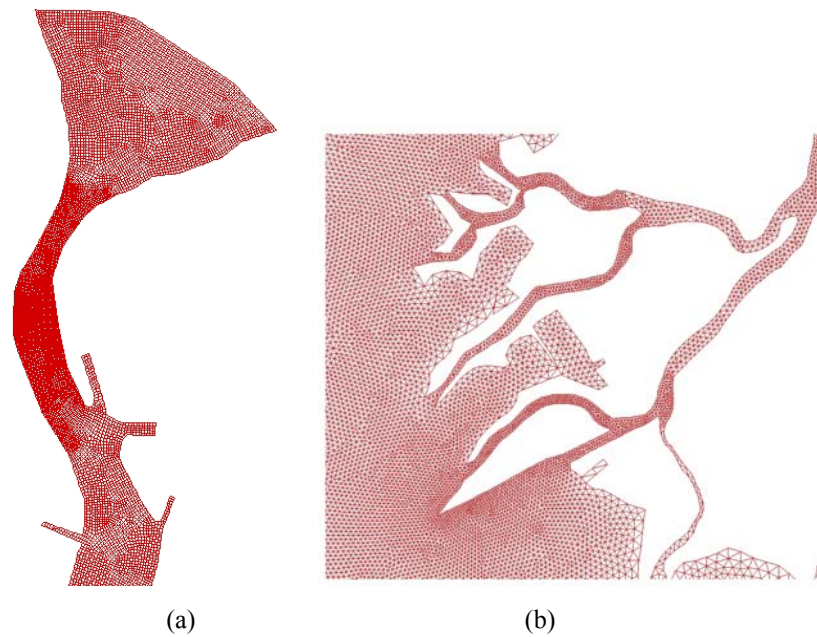


Figure 3. Mesh example for the computational domain: (a) mesh for the Lake Huron inlet area (b) mesh for the delta area in Lake St. Clair

For all three meshes, the simulations were done for 8/24/2005. The bathymetry for year 2005 is from the survey done by USACE. The measured discharge is 5247 m³/s. The numerical results of stages are compared with the measurement along the St. Clair River. From the simulations, the intermediate mesh (mesh ID B) and the fine mesh (mesh ID C) give almost the same results. However, the fine mesh has more double the cell number than the intermediate mesh which makes the computational time much longer. The coarse mesh (mesh ID A) seems not representing the domain and bathymetry well and it gave a result with high level of error. So in the simulations hereafter, the intermediate mesh (mesh ID B) is used.

3. 3D Numerical Model Verifications

HydroSed2D is a two-dimensional model. As all other 2D models, it has its limitations. The major assumption here is the hydrostatic condition. For our case, the St. Clair River is very shallow. The width-depth-ratio is about 40. So the shallow water equation is generally valid. However, at some local areas, such as the first two bends near the inlet, the effects of local features (secondary flow in the bends, the two tongue features etc., see Figure 4) will change the flow from hydrostatic condition. In order to verify if the 2D model give a relative accurate description of our problem, fully 3D simulations were done. The specific purpose of this exercise is to verify that the shear stress in the first two bends given by the 2D model is in the right range.

The three-dimensional numerical code we used is the open source CFD code OpenFOAM v1.5 (OpenCFD, 2008). OpenFOAM is primarily designed for problems in continuum mechanics. It provides a fundamental platform to solve fluid mechanics problems. The core of the code is the finite volume discretization of the governing equations. The Hydrosystems Laboratory at University of Illinois at Urbana-Champaign has used this code in both basic and applied research, such scour around objects (Liu and García, 2008a) and particle settling (Liu and García, 2007).

Due to the limitation of computational resource, only the Lake Huron inlet area and the first two bends are modeled in the 3D simulations. The bathymetry is from the multi-beam scan of Professor Jim Best of University of Illinois at Urbana-Champaign. The 3D view of the 2008 bathymetry is show in Figure 4. The domain is about 8 km long and it has a mesh of around 1.5 million cells. The turbulence is modeled by the k- ϵ model. It takes more than 24 hours for the model to reach steady state in an 8 nodes computer cluster.

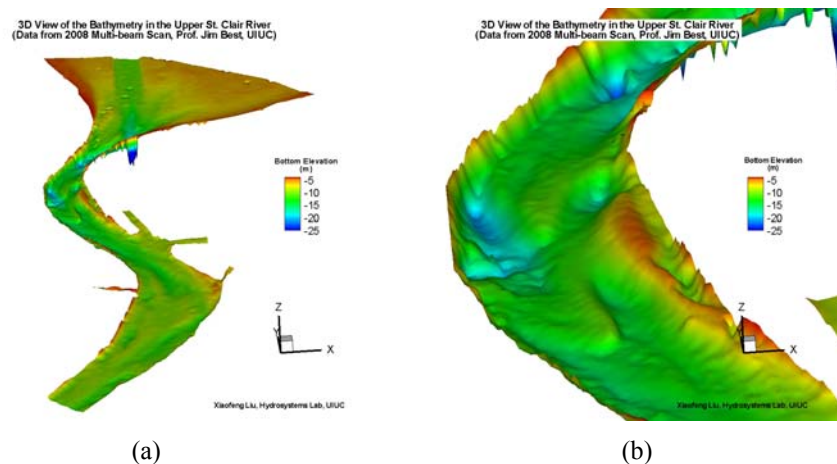


Figure 4. Bathymetry for the upper reach of the St. Clair River: (a) Overall view of the first two bends
(b) Local tongue features at the first bend

The comparison of the bed shear stress between the 2D and 3D models is shown in Figure 5. Although exact match of the shear stresses is not possible, the basic patterns of the shear distribution from both models agree well. For both models, the maximum shear stress is located at

the Lake Huron inlet area and in the second bend, low shear stress is observed. The magnitude of the shear stress also agrees well which means the roughness coefficient we chose and the velocity magnitude the model computed are in the right range. With these, it is safe to say that the HydroSed2D model gives reasonable results.

As an aside, the flow pattern from the 3D model is shown in Figure 6. The stream trace in Figure 6 (a) and (b) helps visualize the flow field. In the first bend, the velocity vectors in several cross sections are shown in Figure 6(c). The secondary flow feature is evident. This might cause the further scour of the deep whole on the outer bend and deposit sediment on the two sand bars in the inner bend. The flow field from the numerical model with 3D ADCP measurement can be used to give a clear picture of what is happening around the bend.

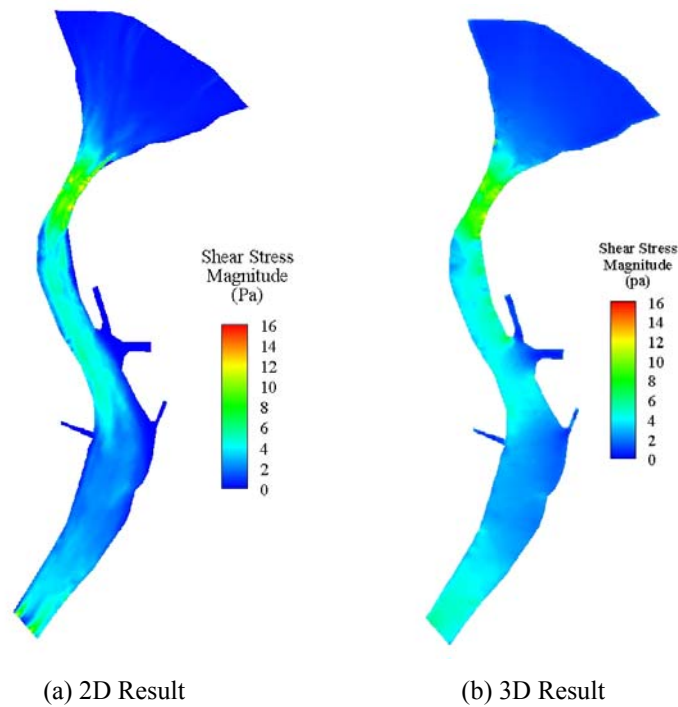
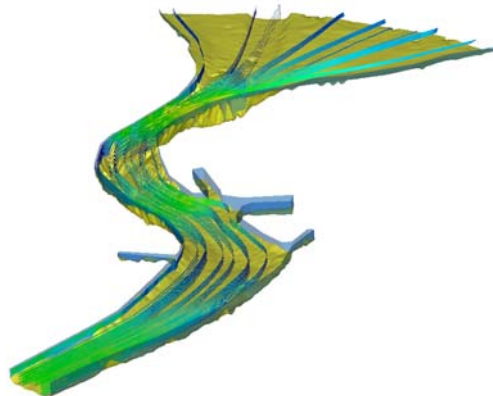


Figure 5. Shear stress comparison between 2D (HydroSed2D) and 3D (OpenFOAM) models



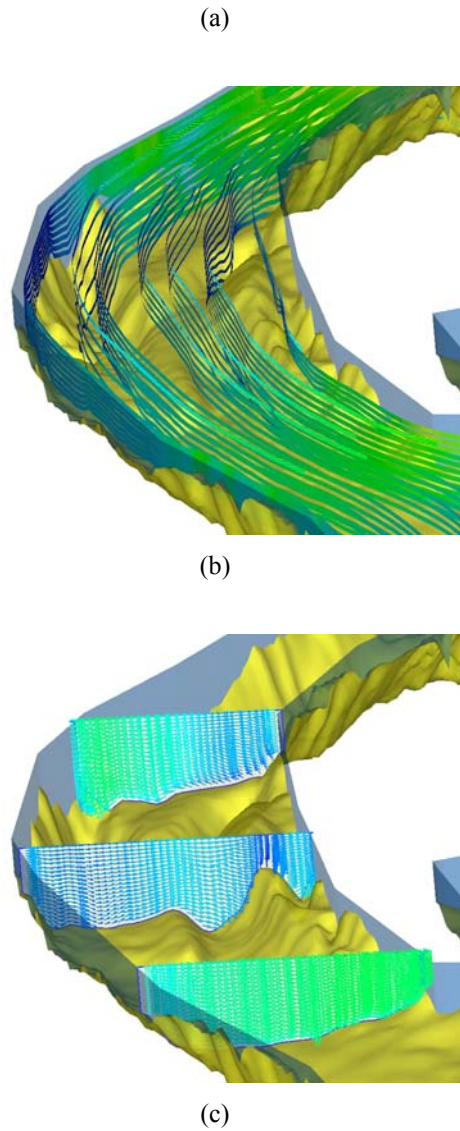


Figure 6. 3D view of the flow field: (a) Overall view of the streamlines (b) Streamlines in the bend (c) Secondary flow features in the bend over the tongue features

4. HydroSed2D Model Applications

Since the model is carefully calibrated and verified, it is used to investigate the possible cause of the continuous dropping the Lake Huron level. Firstly, the shear stress distribution is analyzed and its implication for the sediment transport is deduced. Secondly, the effects of the bathymetry changes on the Lake Huron level are studied. At the end, the model is used to see the effects of the alignment of the Lake Huron inlet channel.

4.1 Shear Stress Distribution

Bathymetry change in the St. Clair River and the sediment transport supply change from Lake

Huron affect the movement of sediment particles. The interaction between the flow and sediment is a coupled process. The river tries to adjust to a new equilibrium after any change. From the under water videos and images, the sediment has a wide distribution of sizes. Depending on the location in the river, the sediment can range from fine sand to very coarse gravels.

Before doing any numerical simulations, some simple calculation can be done to give the average shear stress in the river. Assume the river has a slope $S=2E-5$, water depth $H=10m$, then the average bottom shear stress should be

$$\tau_b = \rho g H S \approx 2Pa$$

Numerical simulations should give an average shear in that order. However, local shear from numerical results could be far apart from this value. In order to see the implications of the shear stress for sediment transport, the critical shear stress needed for the motion of different size of sediment is listed in Table 6. The dimensionless form of this relation, i.e., Shield's diagram, is shown in Figure 7. From this relationship, the average shear stress of 2Pa can only move sediment finer than 5 mm.

The flow condition used for the simulation is the medium discharge condition listed in Table 3. The bathymetry used for the shear stress distribution simulation is from year 2008.

Table 6. Critical shear stress needed for the motion of sediment particles

ψ	D (mm)	Re_p	τ_c^*	τ (pa)
-3	0.125	5.62E+00	3.91E-02	0.08
-2	0.25	1.59E+01	2.20E-02	0.09
-1	0.5	4.50E+01	1.61E-02	0.13
0	1	1.27E+02	1.74E-02	0.28
1	2	3.60E+02	2.11E-02	0.68
2	4	1.02E+03	2.44E-02	1.58
3	8	2.88E+03	2.68E-02	3.46
4	16	8.14E+03	2.82E-02	7.29
5	32	2.30E+04	2.90E-02	15.01
6	64	6.51E+04	2.95E-02	30.49
7	128	1.84E+05	2.97E-02	61.49
8	256	5.21E+05	2.98E-02	123.54

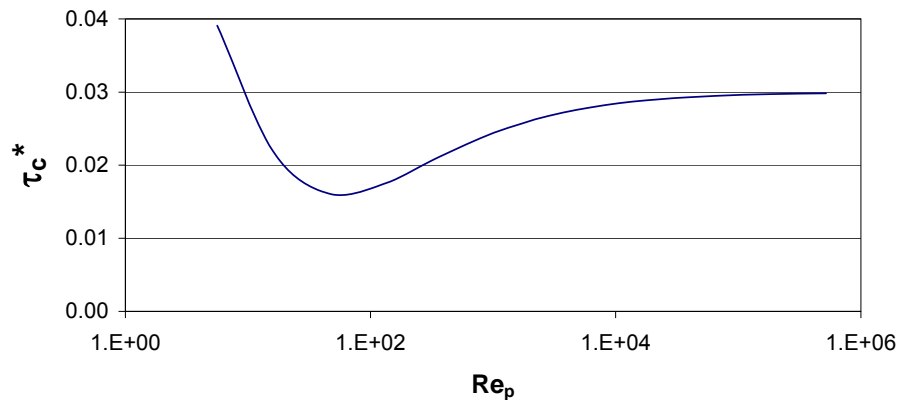


Figure 7. Shield's diagram for the sediment initiation of motion

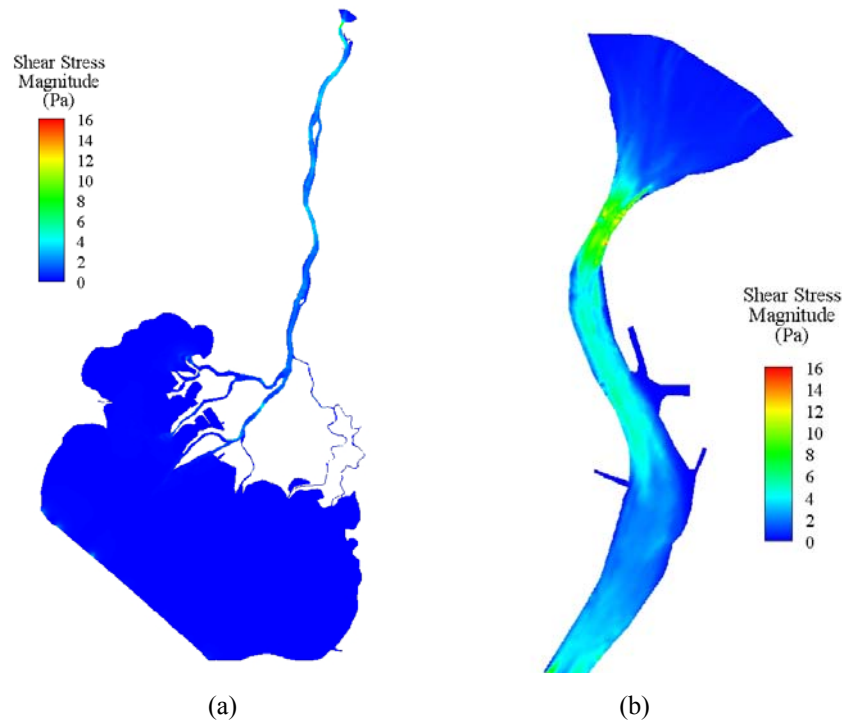


Figure 8. Shear stress distribution in the St. Clair River (medium flow condition): (a) shear stress for the whole system (b) shear stress for the upper reach

The simulation results of the shear stress are shown in Figure 8. High shear stress is only observed from in the St. Clair River channel. In the Lake St. Clair, since the velocity is almost zero, the shear stress diminishes. In the St. Clair River, highest shear velocity is located at the Lake Huron inlet area. In this area, the shear stress is about 8 to 10 Pa. This value of shear stress can move sediment finer than 20 mm diameter. Sediment supply (except extremely big particles) from Lake Huron will be moved across this inlet area and be transported downstream. The very possible deposition location is the in the first bend. In the first bend where there is a deep hole and two big sand bars, the shear stress is around 4 to 5 Pa. This value of shear stress can only move sediment finer than 10 mm diameter. The two sand bars might still be evolving because of relatively high shear stress in this area.

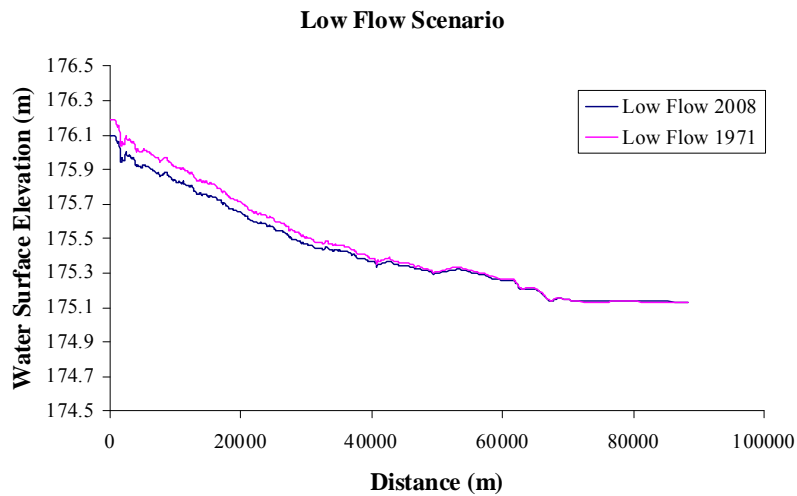
4.2 Bathymetry Change Effects

4.2.1 Two-dimensional Modeling and Analysis

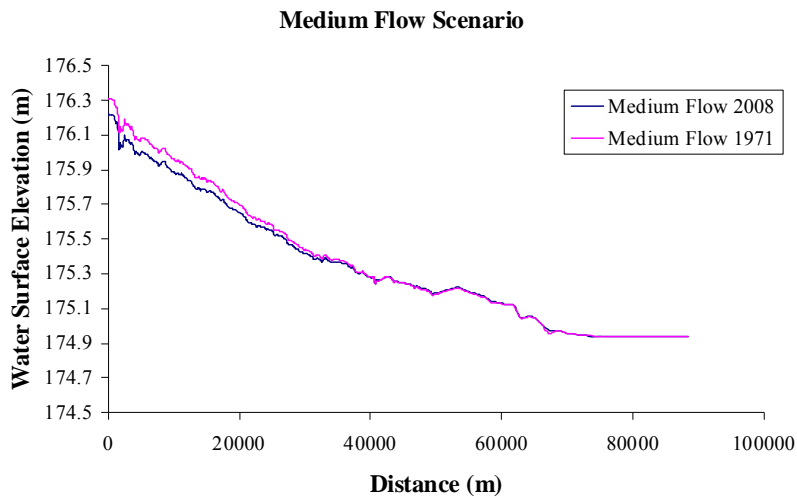
Survey data has shown the bathymetry of the St. Clair River has been modified extensively due to both man made changes and natural processes (such as post-glacial rebound). The bathymetries of 1971, 2000, and 2008 are used to investigate whether the dropping of Lake Huron level is related to the river bottom change. The available bathymetric data include 1971 and 2000 for the full St. Clair River, 2002, 2005, 2006, 2007, and 2008 data for the upper portion of the river, 2002 data for the Lake St. Clair. 2008 data is from the multibeam echo sound mapping by Prof. Jim Best of

University of Illinois at Urbana and Champaign. In this research, for year 1971 and 2000, the data of the whole river of 1971 and 2000, 2002 data for Lake St. Clair, and some data of Lake Huron of 2008 are used. For the year 2008 simulation, the 2008 data for the upper portion of the river, 2000 data for the rest of the river, 2002 data for Lake St. Clair and 2008 data for part of Lake Huron are used. Three sets of hydraulic conditions (low, medium, and high discharges) are simulated (see Table 3).

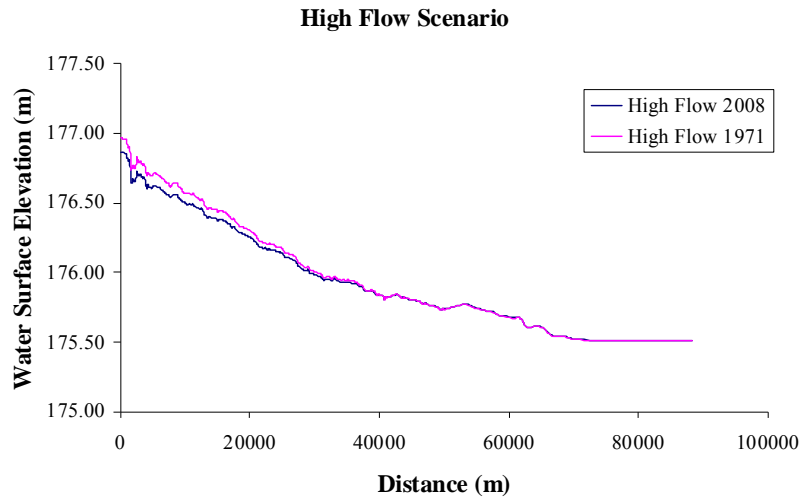
The water surface elevations of the three hydraulic conditions for both 1971 and 2008 are plotted in Figure 9. For all three hydraulic conditions, the bathymetry changes from 1971 to 2008 make the water surface in the whole river system drop. Table 7 lists the Lake Huron water level dropping due to the river bottom change from 1971 to 2008. The level drop is about 9 to 10 cm for all the cases. This number is also consistent with the results from other studies. The dredging and mining in the St. Clair River started from 19th century. If the bathymetry data is available for those years, the dropping of lake level would be even higher.



(a)



(b)



(c)

Figure 9. Comparison of the water surface elevation in the St. Clair River between 1971 and 2008 bathymetry data: (a) Low flow scenarios (b) Medium flow scenarios (c) High flow scenarios

Table 7. Comparison of the Lake Huron level drop between using 1971 and 2008 bathymetry data

Flow Scenarios	Flow Discharge (m ³ /s)	Lake St. Clair Level (m)	Lake Huron Level Drop (m)
Low Flow	4645	175.13	0.094
Medium Flow	5282	174.94	0.089
High Flow	6006	175.51	0.098

4.2.2 One-dimensional Backwater Curve Analysis

The St. Clair River is long (~80km) and shallow (width/depth~40). It is believed that even without 2D and 3D numerical models, 1D back water calculation can give some estimation of the water surface change due to bathymetry changes. If one looks at the bathymetry changes from 1948 to 2000 in Figure 10, the major part of the river bottom is been lowered by about 30-50 cm. At the upstream and downstream ends, the river bottom has been dredged for about 3-4 meters due to the 27 feet navigation requirement. According to this, some scenarios of 1D back water curve calculations are done. There scenarios are dredging 4 meters in the downstream 10 km, midstream 10 km, upstream 10 km, and upstream+downstream dredging combined. The river is assumed to be 80 km long, has a slope of 2E-5, and water depth in the Lake St. Clair is fixed at 10 meters.

Figure 11 shows the 1D back water calculation results. For all the cases, no matter where the dredging is taking place, the water surface elevation in the river always goes down. This is true since for a river like this, the mean Froude number is about 0.1, which means the whole river is subcritical. Any change in the St. Clair River will affect the water surface both downstream and upstream. In order to see clearly the effect of dredging, Figure 12 plots the original water surface without dredging and the water surface after both upstream and downstream 4 meters dredging

which is similar what happened in St. Clair River.

Quantitatively, Table 8 lists the Lake Huron level dropping from the 1D back water curve calculation. For all upstream, midstream, downstream dredging, the Lake Huron level drops about 15 cm. If upstream and downstream dredging combined, the Lake Huron level drops about 29 cm.

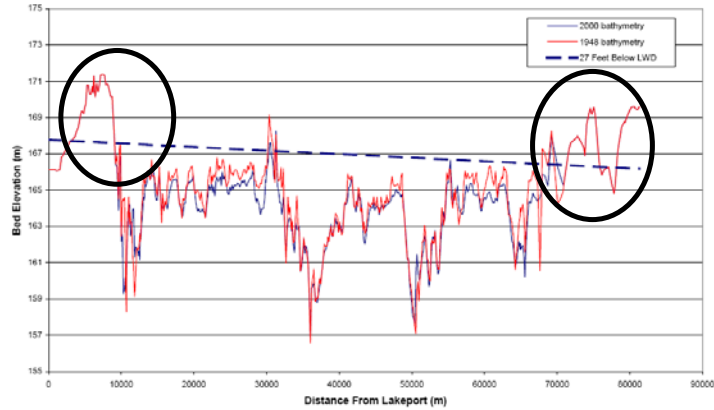
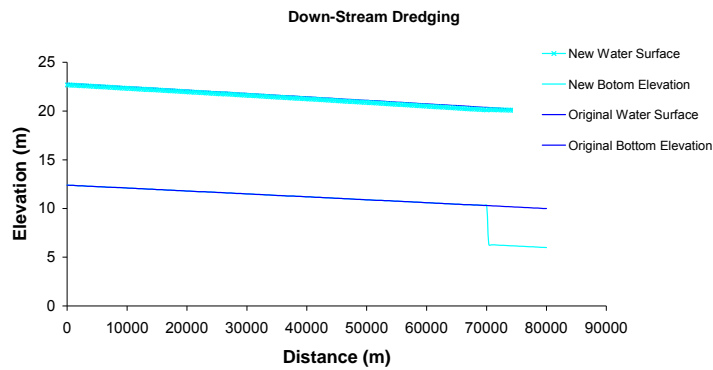
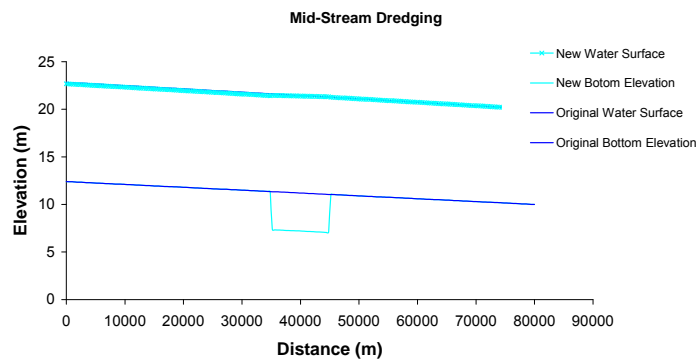


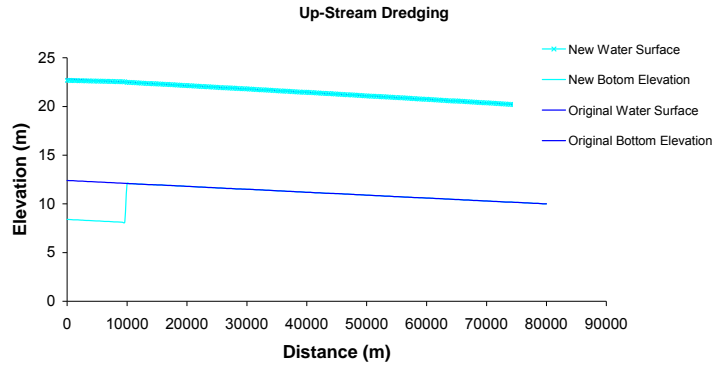
Figure 10. Dredging and bathymetry changes along the St. Clair River (adapted from Baird & Associates, 2005)



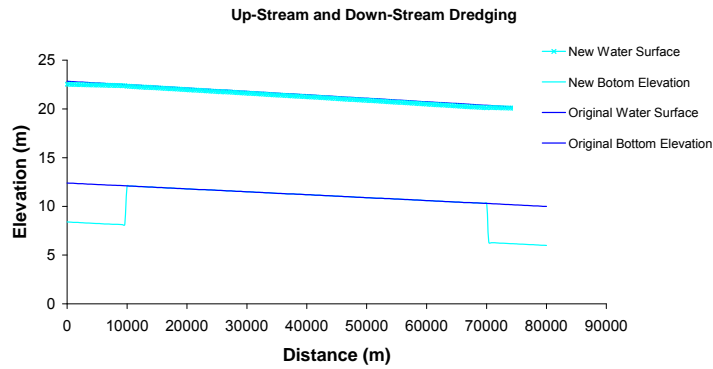
(a)



(b)



(c)



(d)

Figure 11. Dredging Effects on the Water Surface Elevations: (a) Downstream Dredging (b) Midstream Dredging (c) Upstream Dredging (d) Upstream/Downstream Dredging Combined

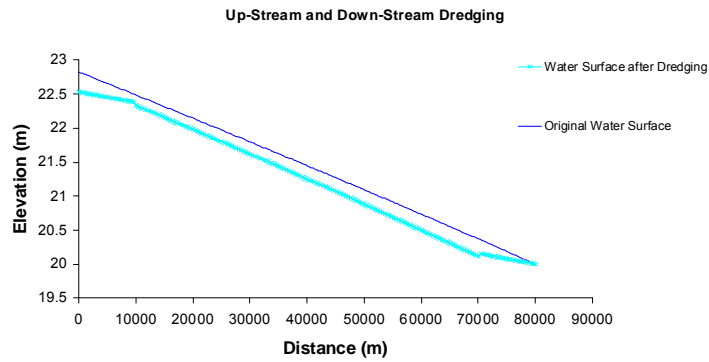


Figure 12. The original water surface and the water surface after both upstream and downstream dredging

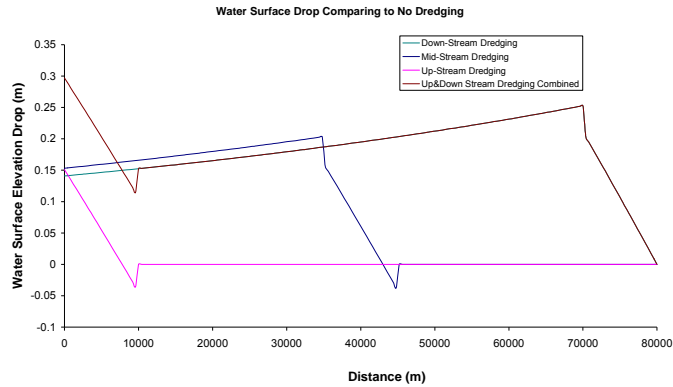


Figure 13. Water Surface Drop due to Bathymetry Changes

Table 8. Effects of Bathymetry Changes on the Lake Huron Level
(1D Back Water Curve Calculations)

Bathymetry Changes	Lake Huron Elevation Decrease (m)
Downstream Dredging	0.141
Midstream Dredging	0.153
Upstream Dredging	0.151
Upstream + Downstream Dredging	0.297

4.2.3 Two-lake Problem and Conveyance Change Analysis

The St. Clair River is a canal connecting two lakes, namely Lake Michigan-Huron and Lake St. Clair. The bottom slope of the St. Clair River is negligible. The upper portion of the river even has a negative slope. Therefore the discharge in the river is mainly driven by the level difference between the lakes. This is a typical example of canal delivery of subcritical flows (see Chapter 11 of Chow 1959). Figure 14 shows the scheme of the two-lake problem. Although it is not possible to follow the same analysis in Chow (1959), HydroSed2D is used to generate the Hydraulic Performance Graph (HPG) with the bathymetry of 1971 and 2007.

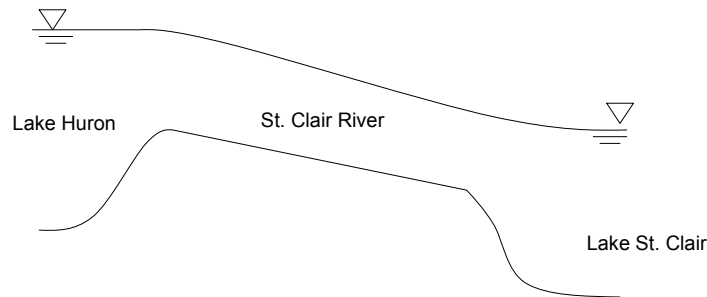


Figure 14. Scheme of the two-lake problem applied to the Lake Huron, St.Clair River, and Lake St. Clair system

Discharge Q constant curves are plotted in Figure 15 for the bathymetry of year 1971 and 2007. For a given combination of Lake Huron and Lake St. Clair levels, a discharge in the St. Clair

River can be obtained from the 2D model. 33 simulations were done for each bathymetry, which results in 66 simulations for year 1971 and 2007. From the comparison, the conveyance has increased from 1971 to 2007. For the same combination of lake levels, the discharge is higher for year 2007 than for year 1971. It is also found that the conveyance change is larger when the lakes have higher water levels.

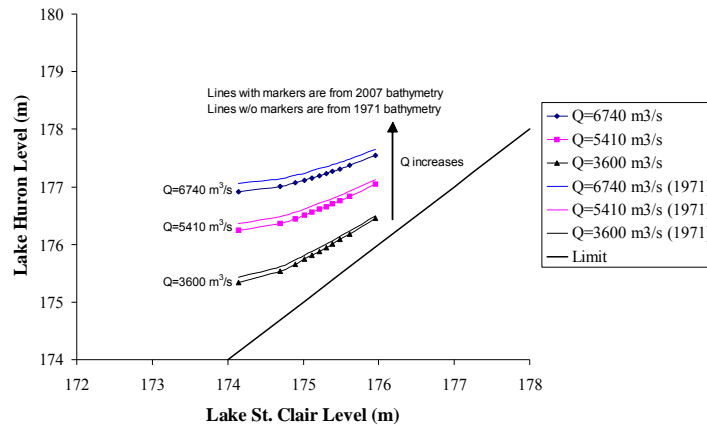


Figure 15. Q constant curves for year 1971 and 2007 as a function of Lake Michigan-Huron and Lake St. Clair Levels. Smooth lines are results for 2007 and lines with markers are for 1971.

The conveyance change in the St. Clair River is used to estimate its effect on the lake levels. The question needs to be answered is how long the Lake Michigan-Huron level will drop 0.8 m assuming there is an increase in the St. Clair River conveyance. Also assumed is that everything else is kept constant (e.g., precipitation, evaporation, etc.). The purpose is to see how relevant the conveyance change is and to what extend.

The calculation results are shown in Table 9. For 0.5%, 1%, and 5% changes of the St. Clair River conveyance, it takes 110, 55, and 11 years to lower the lake level by 0.8 m. In that sense, the water level in Lake Michigan-Huron is sensitive to the conveyance change in St. Clair River. A small percentage increase of conveyance will drop the lake level very quickly (in the order of 10-100 years). As a matter of fact, it only takes the mean discharge (5410 m³/s) about 50 years to drain all the 8,458 km³ volume of water in the Lake Michigan-Huron system without any inflow. To put things into perspective, it is beneficial to make the following analogy. Lake Michigan-Huron is like a big bath tub full of water. However, it also has a very big drain hole (the St. Clair River). Small percentage change of the drain hole could fluctuate the water level in the bath tub quickly to some substantial extend.

Table 9. Time needed for the Lake Michigan-Huron level to drop 0.8 m (assuming everything else is kept constant). Different conveyance changes are also assumed.

Area of Lake Michigan-Huron (km ²)	Water Level Drop (m)	Water Volume Loss (m ³)	St. Clair River Average Discharge (m ³ /s)	0.5% Conveyance change (m ³ /s)	1% Conveyance change (m ³ /s)	5% Conveyance Change (m ³ /s)
117,702	0.8	9.42E+10	5410	27	54	271
				Time needed (years)	Time needed (years)	Time needed (years)
				110	55	11

4.3 Lake Huron Inlet Alignment Effects

In Baird & Associate (2005), one possibility of Lake Huron level drop is identified as the inlet channel alignment. In Figure 16, the bathymetries of year 1929 and 2000 are plotted. The inlet channel is shifted from east Canada side to the west US side in the part several decades. If comparing to the 2008 bathymetry data, the deep inlet channel is shifted even more toward west.

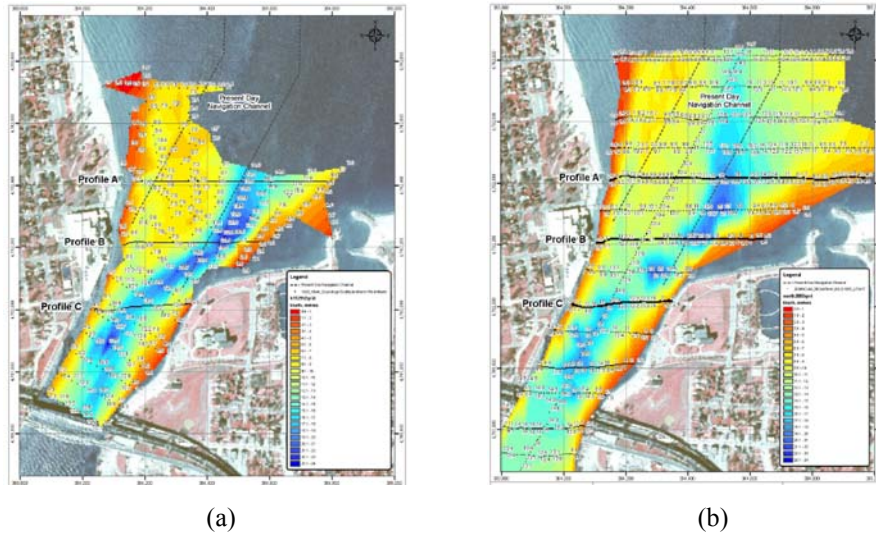
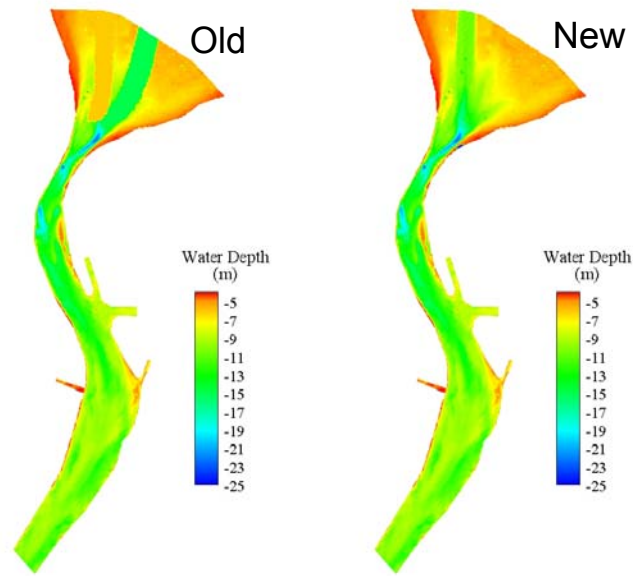


Figure 16. Bathymetry at the Lake Huron inlet area (adapted from Baird & Associate, 2005):
(a) 1929 (b) 2000

In order to see whether this inlet alignment change will affect the Lake Huron level, simulations were done using the old bathymetry where the deep inlet channel is placed toward the east side (see Figure 17). This bathymetry is obtained roughly according the figures in Baird report.

There is no major change of shear stresses distribution due to the inlet alignment change (see Figure 18). The major change is focused in the Lake Huron area. The velocity distribution changes a little bit due to the change of inlet alignment (see Figure 19). Velocity changes mainly happen in the Lake Huron area. For the rest of the river, the velocity is not affected. In terms of Lake Huron level, the new bathymetry even raised the Lake Huron elevation by 3mm (see Figure 20). This is reasonable since for the current bathymetry (year 2008, for example), there is a larger angle between the inlet channel and the St. Clair River. This angle increases the resistance force and the water has to spend some energy to adjust its direction before flows into the river.



(a)

(b)

Figure 17. The bathymetries used for the inlet alignment study: (a) Old bathymetry where the inlet is toward the east side (b) New bathymetry where the inlet is toward the west side

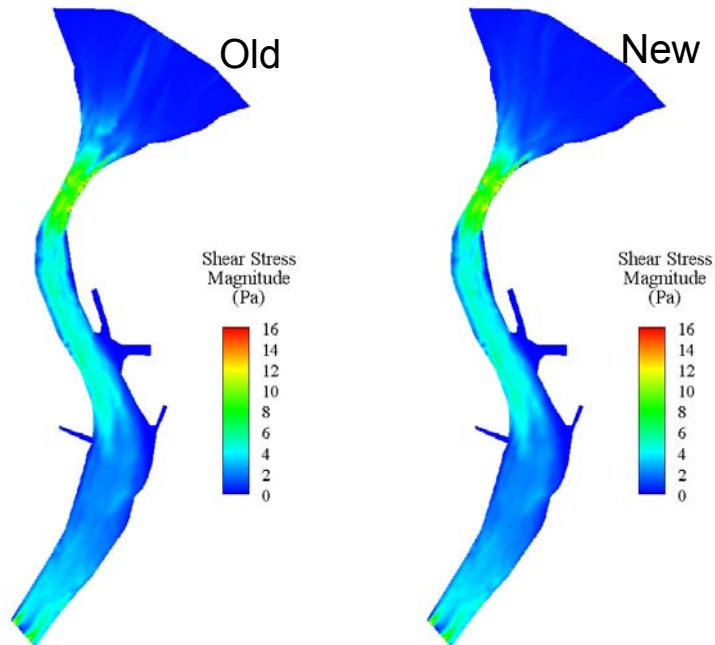


Figure 18. Effects of the inlet alignment on the bottom shear stresses: (a) old bathymetry where the inlet is toward the east side (b) new bathymetry where the inlet is toward the west side

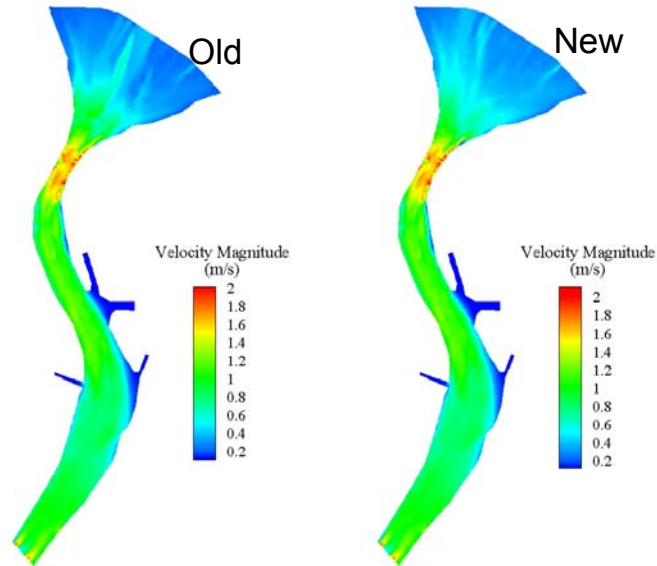


Figure 19. Effects of the inlet alignment on the velocity distribution: (a) old bathymetry where the inlet is toward the east side (b) new bathymetry where the inlet is toward the west side

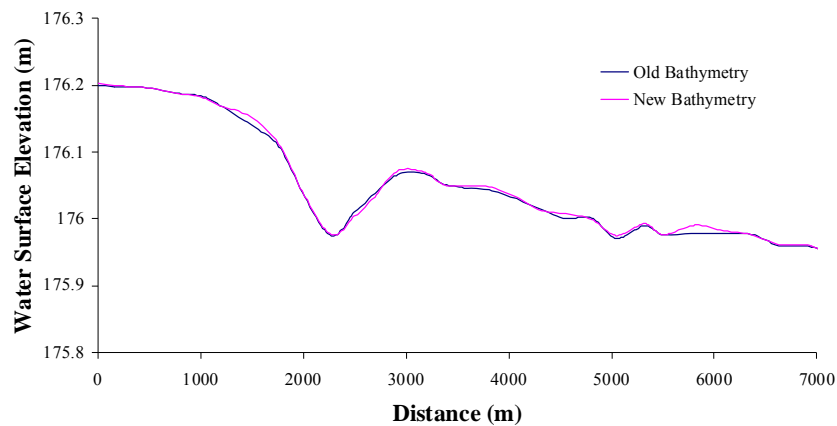


Figure 20. Effects of the inlet alignment on the water surface elevation in the St. Clair River (the new bathymetry even raised the Lake Huron Level by 3 mm)

5. Sediment Transport and Armoring Analysis

5.1 Gravel Transport

The formula used to do the computation is from Parker (1990), which is implemented in a Microsoft Excel file which can be downloaded from <http://vtchl.uiuc.edu/people/parkerg/>. This

surface-based bedload transport relation for gravel excludes sand. The finest size of the sediment must be greater than 2 mm. The details of the program can be found in the website and the companion notes. The original program Acronym1 has three different versions: Acronym1, Acronym1_R, and Acronym1_D.

Acronym1 is used to compute the volume bedload transport rate per unit width and the bedload grain size distribution from a specified surface grain size distribution (with sand removed), a bed shear stress, and a specific gravity of the sediment. Acronym1_R uses the Manning-Strickler relation for flow resistance. Given flow discharge, channel width, and channel slope, it first calculates the bed shear stress assuming normal flow condition. Then the same code in Acronym1 is used to calculate the transport rate. Acronym1_D combines the scheme of Acronym1_R with a flow duration curve. The bedload transport rate and bedload grain size distribution are computed for each flow of the curve, and then averaged to yield a mean bedload transport rate and a mean bedload grain size distribution.

In this study, since HydroSed2D is used to calculate the shear stresses on the river bed, normal flow assumption is not necessary. The general analysis process is as follows. After the calibration in the previous section, HydroSed2D is run to get the shear stress distributions under different flow conditions. These flows cover the whole flow duration curve for the river as shown in Figure 21. The flow duration curve is calculated through the monthly averaged flow data from 1963 to 2006. For each flow condition, the shear stresses on the bottom at the 9 river transects (see Figure 22) are extracted. The bed material size distributions at the corresponding cross sections are provided by Environment Canada through the video image analysis. Figure 23 shows the grain size distributions for the different transects analyzed. It is assumed that the given grain size distribution applicable across the entire cross-section. With these as inputs, the Acronym code is run for all the cross sections. Figure 24 shows the general process of combining the HydroSed2D and Acronym code.

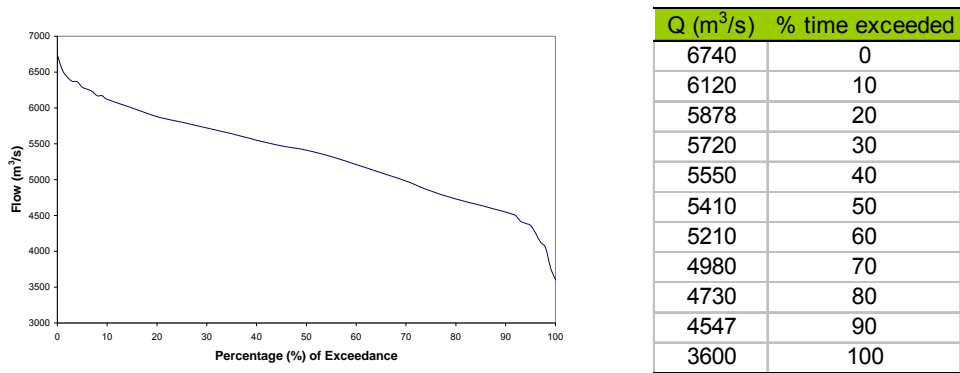


Figure 21. Flow Duration Curve for the St. Clair River
(Monthly Average Discharge from 1963 to 2006)

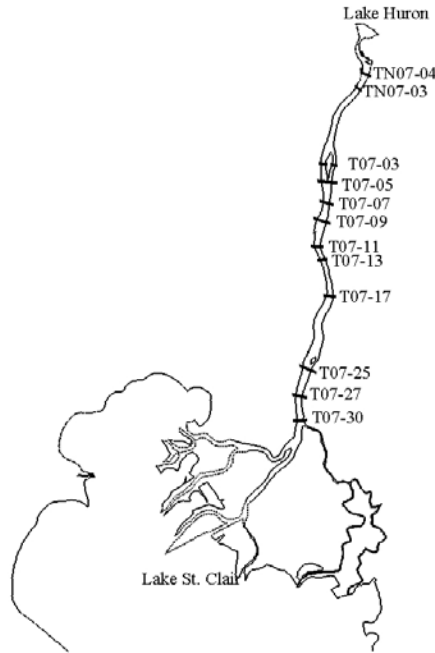


Figure 22. Transects along the St. Clair River

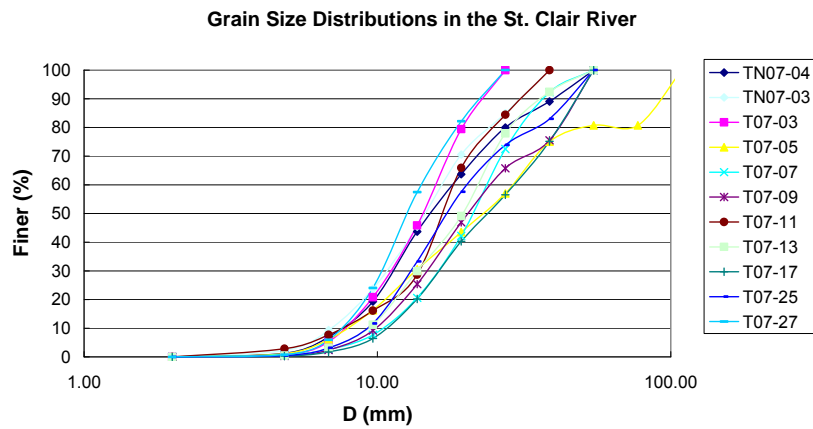


Figure 23. Grain Size Distributions in the St. Clair River for Different Transects

For each transect, it is divided into many small sections as in Figure 25. For section i , the shear stress is the average values at the end points which define this section. The transport rates are calculated at each of these sections and an average value is computed for the whole transect. Since the run of Acronym1 code will be repeated for many times, the original code is modified to run in batch mode. Specifically, 11 flows are used to cover the whole flow duration curve and 9 transects are analyzed. For each transect, it is divided into 50 small sections. Therefore, the Acronym code is called $11 \times 9 \times 50 = 4950$ times.

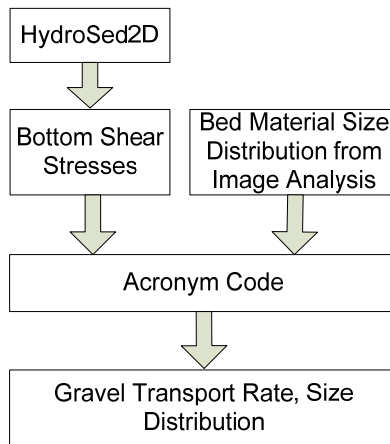


Figure 24. Analysis Process for the Gravel Transport Calculation

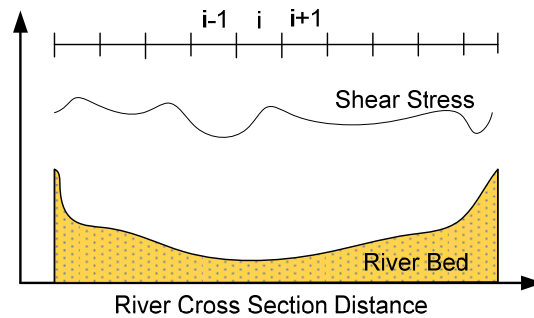


Figure 25. Division of the River Cross Section

TN07-04 is chosen as a typical transect whose calculation results are elaborated. Results for other transects are shown in the Appendix. Figure 26 shows the river bottom shear stress distribution across the transect TN07-04 for the discharge of $5410 \text{ m}^3/\text{s}$, which corresponds to 50% on the flow duration curve. The shear stresses range from 3 to 5 Pa, which is not high even this transect is located upstream of the river. Figure 27 shows the size distributions of the sediment in the surface and bedload. The surface geometric mean of the sediment size is 16 mm and the bedload geometric mean is about 9.9 mm. The ratio between them is about 1.62. The river renders itself able to transport the coarse half of its gravel load at the same rate as its finer half by overrepresenting coarse material on its surface, where it is available for transport. The mean annual volume bedload transport rate per unit width for transect TN07-04 is about $1.07 \times 10^{-11} \text{ m}^2/\text{s}$, which is negligible. This translates to an also negligible annual sediment yield of about 0.54 ton (the river width at this transect is about 600 meters).

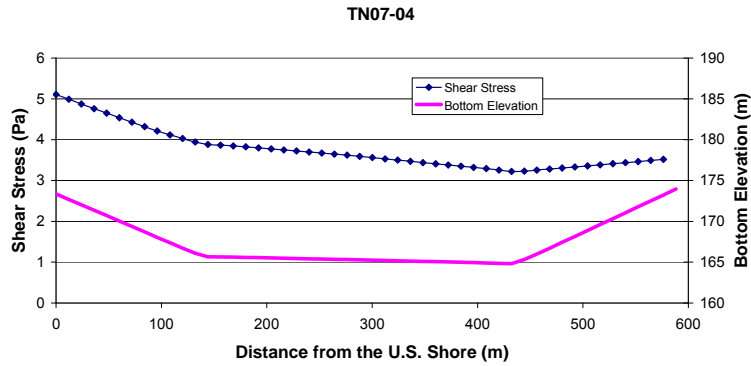


Figure 26. Shear Stress Distribution and River Bottom Elevation for Transect TN07-04 for Discharge of $5410 \text{ m}^3/\text{s}$ (Corresponding to 50% on the Flow Duration Curve)

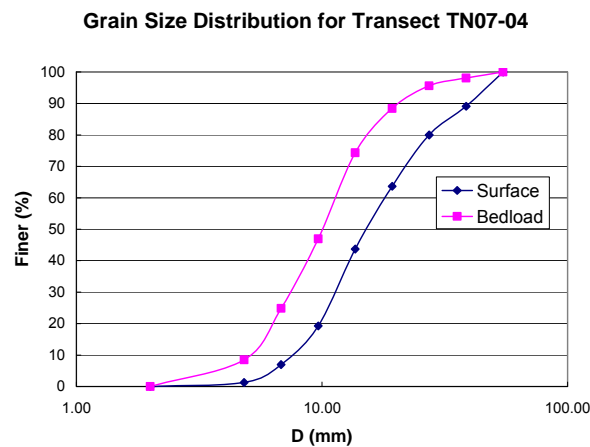


Figure 27. Mean Surface and Bedload Grain Size Distributions for the Transect TN07-04

Through the analysis of all transects, some general conclusions can be drawn for the St. Clair River.

- Although upstream of the river seems to move more sediment than downstream, it is found that the capacity of the river to move gravel-sized material at all transects is extremely limited. The mean annual bedload transport rate we obtained was (for all practical purposes) zero. The effective Shields number was about 0.004 to 0.015, i.e. less than the smallest reasonable guess for a critical Shields number. The results are listed in Table 10 and Table 11.
- The bed should be armored. If the lack of imbrication can be taken as evidence for the lack of armoring, one should look for causes other than significant bedload transport for this: ship propeller wash, ice, bioturbation, etc. Perhaps the first and the second are more likely which will be discussed later.
- One can also make some quick inferences through simple analysis. The bed elevation profile from Fort Gratiot to Port Lambton (42 km reach) shows lots of local variation, but no consistent trend from which we can extract a bed slope (see Figure 28). The linear fitting of the bed long profile shows a

negligible slope of 2×10^{-5} . We might as well consider this bed slope to be zero, and the flow to be driven entirely by the water surface gradient. The water surface slope shows a significant decline in the downstream direction, with a value near 2.9×10^{-5} for the upper half and 1.5×10^{-5} on the lower half (see the previous sections). The implication is that the shear stresses upstream should be somewhat higher than downstream. This downstream decreasing of shear stress is evident in Figure 29, which shows the river center shear stresses. Despite a small reach in the upstream, the computed shear stresses are in the range of 2 - 6 Pa. Considering the mean size of gravel material (12 mm to 23 mm), the Shields numbers should not be higher than about 0.03. Again, this implies a very limited capacity to move gravel.

- The calculations so far do not support global mobility of the gravel. The variations in cross-sectional shape and alignment support the possibility of local “clear water scour”. Below Dickenson Island, the shear stress drops even lower, i.e. ~ 2 Pa. The photo images show a sand bed here, but we don’t know the sizes. Having said this, even if we assume a grain size of 0.5 mm, we obtain Shields numbers that are about 1/8 of typical sand/bed rivers at bankfull flow. So the capacity to move sand does not seem very high, either.
- The local “tongue-like” feature of bed forms at the first two upstream bends does not contradict the global immobility of the gravel. In general, the upstream of the river, especially in the Lake Huron inlet contraction area, the shear stresses are relatively high than the rest of the river. Annual sediment yield across transects in this region is about 0.5 to 1 ton. The “tongue-like” feature has a total of about 10 to 100 tons of sand/gravel. The calculated sediment yield is enough to generate, sustain, and even transform this feature over a period of 10 to 50 years. Local flow conditions due to secondary flow in the bend, ship maneuver, ice cover/ice jam, etc., shall also contribute to some extent.
- For the long-term morphodynamic simulation of bed evolution along the St. Clair River, it is not possible at current stage because of the lack of data for grain size distributions in enough details. The calculations to date, however, do not even warrant such a computation. In the long term, the river is likely stable in the overall sense. (Again, we are considering a scale larger than e.g. scour associated with ships sinking.)

Table 10. Geometric Mean of Sediment Size for Surface and Bedload

Transects	TN07-04	T07-03-Left	T07-05	T07-07	T07-09	T07-11	T07-17	T07-25	T07-27
Mean annual volume bedload transport rate per unit width $qbTa$ (m^2/s)	1.072E-11	3.938E-13	1.065E-18	1.083E-15	7.970E-19	9.106E-15	2.591E-17	8.714E-19	1.410E-15
Mean annual Shields number based on surface geometric mean size tga^*	0.015	0.012	0.005	0.009	0.005	0.010	0.006	0.004	0.008
Mean annual shear velocity u^*a	0.06188	0.050	0.044	0.053	0.041	0.050	0.045	0.036	0.041

Table 11. Gravel Transport Analysis Results

Transects	TN07-04	T07-03-Left	T07-05	T07-07	T07-09	T07-11	T07-17	T07-25	T07-27
Mean annual volume bedload transport rate per unit width qb_{Ta} (m^2/s)	1.072E-11	3.938E-13	1.065E-18	1.083E-15	7.970E-19	9.106E-15	2.591E-17	8.714E-19	1.410E-15
River Width (m)	600	500	1080	600	990	625	700	900	640
Annual Sediment Yield (ton)	5.38E-01	1.65E-02	9.62E-08	5.44E-05	6.60E-08	4.76E-04	1.52E-06	6.56E-08	7.55E-05
Mean annual Shields number based on surface geometric mean size tga^*	0.015	0.012	0.005	0.009	0.005	0.010	0.006	0.004	0.008
Mean annual shear velocity u^*a	0.06188	0.050	0.044	0.053	0.041	0.050	0.045	0.036	0.041

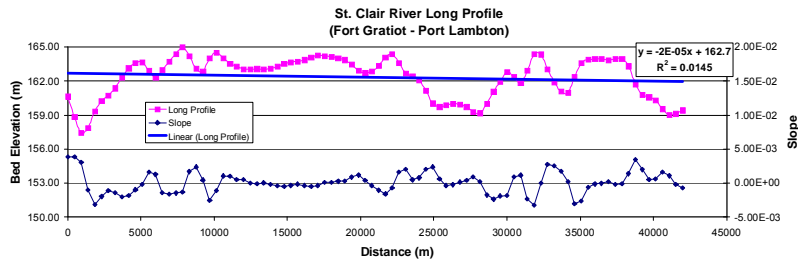


Figure 28. St. Clair River Long Profile and Bottom Slope from Fort Gratiot to Port Lambton

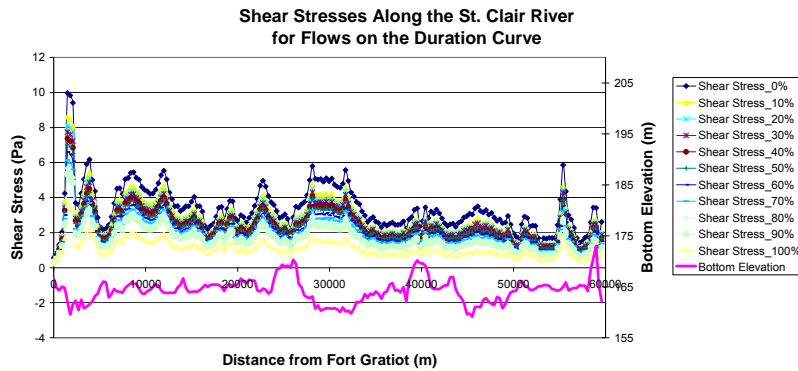


Figure 29. Shear Stresses along the St. Clair River for Flows on the Duration Curve

5.2 Sand Transport

Sand patches have been observed along the St. Clair River. In the upstream, both sides of the river have sand covers due to the sand feed from the shore of the Lake Huron. In the downstream, sand cover expands to larger portion of the cross section. In the delta region into the Lake St. Clair, sand might cover the whole area. In this section, sand transport rate is estimated and its impact on the conveyance is analyzed. To be specific, the theoretical sand transport rate q_s is calculated assuming the whole cross section is covered by sand. Then the sand coverage P_0 for each cross section is estimated by inspecting the under water video images. Finally, the actual sand load q_{sl} is back calculated using the formula

$$P_0 = \frac{q_{sl}}{q_s}$$

Sand size analysis has been done using the grab samples taken in various locations along the river. Table 12 shows the sand size results for three cross sections which represent the upstream, middle, and downstream of the river bed. For each cross section, samples were taken at left bank, middle, and right bank, which are distinguished by “A”, “B”, and “C” in the location names. Some cross sectional variations of sand sizes have been observed. For the upstream section, sand patches are located along the side of the river which is evident from the under water videos. The sand has a D_{50} ranging from 340 to 570 microns. In the middle reach of the river, the sand has a D_{50} of about 200 to 300 microns. Very fine sand with D_{50} of 50 to 80 microns has been retrieved from the downstream section. This is consistent with the general downstream fining trend of typical river systems. Despite the variations in the sand size both along the river and across the transect, two typical sand sizes (0.5 mm and 1 mm) are used to calculate the sand transport rates.

Table 12. Sand size results from the grab samples taken for three typical (upstream, middle, and downstream) cross sections

Location	TN07-03A	TN07-03B	TN07-03C	T07-10A	T07-10B	T07-10C	T07-25A	T07-25B	T07-25C
D_{50} (μm)	569	2409	343	375	204	7768	50	1548	83

The method to determine the sand cover percentage for each transect is through the inspection of the under-water videos. These videos were played and the types of sediment cover and vegetations were recorded. Each category is assigned a percentage number which describes the sand coverage. Since the UTM coordinates are recorded on the video image, the length of each sediment cover category can be calculated and therefore a cross-section averaged sand coverage. As an example, Figure 1Figure 30 shows the four different bed material coverage for transect TN07-03. In Table 13, the process of calculation of sand coverage for the entire transect TN07-03 is illustrated. The calculations for other transects are similar.

Three typical transects are selected for the sand transport rate calculation, namely TN07-03, T07-09, and T07-27, which represent upstream, middle, and downstream portion of the river respectively. The sand coverage values for these three transects are about **0.12**, **0.32**, and **0.5** respectively.

The calculation process for the sand transport rate Q_s is similar to the one used for the gravel transport. The shear stress distributions for each transect covering the flow duration curve are from the *HydroSed2D* model. The Engelund-Hansen (1976) sand transport formula is used, which has the form

$$q^* = \frac{0.05}{C_f} (\tau^*)^{\frac{5}{2}}$$

where $q^* = q_s / (\sqrt{RgDD})$ is the dimensionless sediment transport rate, R is the submerged

specific gravity of the sediment, g is the gravitational acceleration, D is the mean diameter of the sand, C_f is the friction factor, $\tau^* = \tau / (\rho g R D)$ is the Shield's number.

Table 14 shows the calculation results of sand transport rate Q_s (assuming full sand coverage) and estimated sand load Q_{sl} (back calculated = $P_0 * Q_s$).

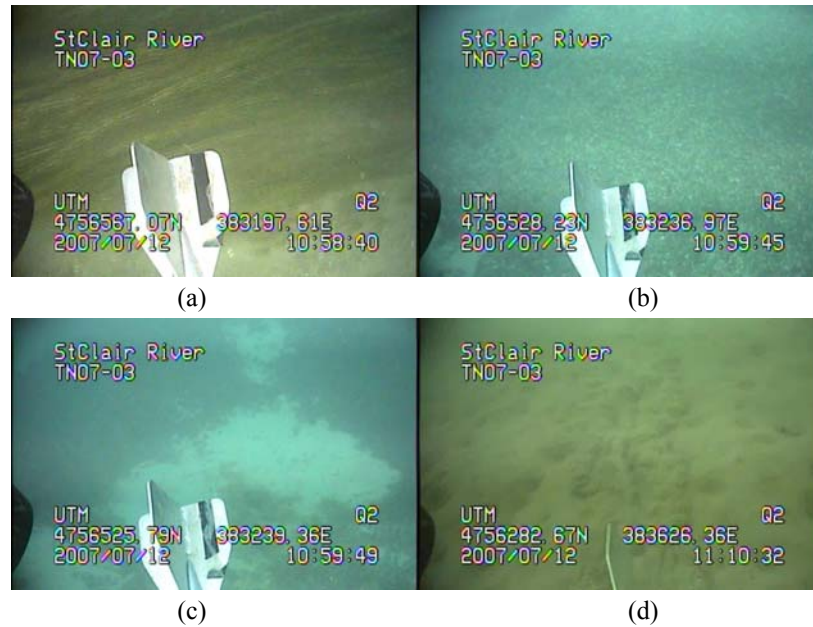


Figure 30. Images of different sand coverage for the transect TN07-03: (a) Vegetation dominant (b) Small gravel dominant (c) Thin layer of gravel on top of bed rock (d) Sand dominant

Table 13. Example calculation of sand coverage for transect TN07-03

Image Number	UTM Coordinates North	UTM Coordinates East	Distance	Sand cover percentage	Distance*Sand_Cover	Description
0	4756580	383189	0	0		start
1	4756578	383189	1.94	0	0.00	vegetation
2	4756566	383197	16.12	0	0.00	vegetation
3	4756524	383240	75.74	0.2	11.92	small gravel with algae, some wood debris, some bed rock exposure
4	4756292	383622	520.03	0.1	44.43	small gravel with a lot of shells (shells are not moving), some bed rock exposure, the layer of gravel is very thin
5	4756282	383623	526.46	0.9	5.79	sandy and muddy bed, the bed is easily disturbed
				Average sand coverage P_0	0.12	

Table 14. Sand transport rate Q_s (assuming full sand coverage) and sand load Q_{sl} (back calculated= $P_0 * Q_s$) for each transect

D_{50} (mm)	TN07-03			T07-09			T07-27		
	P_0	Q_s (Mt/yr)	Q_{sl} (Mt/yr)	P_0	Q_s (Mt/yr)	Q_{sl} (Mt/yr)	P_0	Q_s (Mt/yr)	Q_{sl} (Mt/yr)
0.5	0.12	5.80	0.70	0.32	2.30	0.74	0.50	2.50	1.25
1	0.12	1.45	0.17	0.32	0.58	0.19	0.50	0.58	0.29

From Table 14, even though the sand load Q_{sl} in the upstream and middle of the St. Clair River is less than that of the downstream, one can not conclude that the downstream portion of the river is under degradation. The reason simply lies in the fact that the estimation in Table 14 includes a large error margin. The sand coverage derived from the underwater video is rough and the change of this value could alter the conclusion completely. As a demonstration, the average sand load Q_{sl} along the river is about $(0.70+0.74+1.25)/3 = 0.89$ Mt/yr for $D_{50} = 0.5$ mm. If assuming the whole river is in equilibrium sand transport state, i.e., the amount of sand coming into the river equals that going out. It is also assumed that this equilibrium sand load is 0.89 Mt/yr which is the average calculated sand load. The required sand coverage and the original ones are shown in Table 15. It is clear that the change of sand coverage is not so high. With the large error margin of the sand coverage values derived from the videos, it can be concluded that the river sand transport might be in the equilibrium state and it will not affect the overall hydraulics of the river. Moreover, nowhere along the river is fully covered by sand, which means the river is under capacity in transporting sand. This further confirmed that the sand has minor effect on the hydraulics of the river.

Table 15. Demonstration of the sensitivity of the sand coverage P_0 . The result (for $D_{50} = 0.5$ mm) shows a small change of sand coverage P_0 could alter the conclusion.

Sand Coverage	TN07-03			T07-09			T07-27		
	P_0	Q_s (Mt/yr)	Q_{sl} (Mt/yr)	P_0	Q_s (Mt/yr)	Q_{sl} (Mt/yr)	P_0	Q_s (Mt/yr)	Q_{sl} (Mt/yr)
Original	0.12	5.80	0.70	0.32	2.30	0.74	0.50	2.50	1.25
Changed	0.154	5.80	0.89	0.39	2.30	0.89	0.36	2.50	0.89

5.3 Glacial Till Erosion Test and Analysis

(To be finished by Jose Mier)

6. Ice Cover and Ice Jam Effects

Ice cover and ice jam affect the sediment transport in a river on different time and spatial scales (chap 13 of García, 2006). Generally, for long time and large spatial scales, the ice cover/ice jam will increase and redistribute river channel's resistance and reduce the sediment transport rate. However, on the local scale, an ice cover can redistribute the flow laterally which may cause both sediment scour and deposition. During the surge of water and ice following an ice jam breakup, the water discharge and sediment transport rate can jump to a relatively high value. Although a lot of researches have been done, these postulations about the ice effect are still not fully verified. In this section, the effects of ice cover and ice jam are briefly reviewed. The interpretations for the St. Clair River are also provided.

6.1 Flow Redistribution Effect under an Ice Cover

The shallow portion of a cross section usually has low flow velocity and it provides a place for the ice frazil to accumulate (Figure 31 **Figure 31 Flow redistribution in a river cross section**

(adapted from Ettema and Daly, 2004)). This will block the flow in the shallow area and focus it to the deep portion. Higher velocity there might cause sediment scour and further deep the channel. This may contribute to the deep the whole in the first bend when there is an ice cover on top of it.

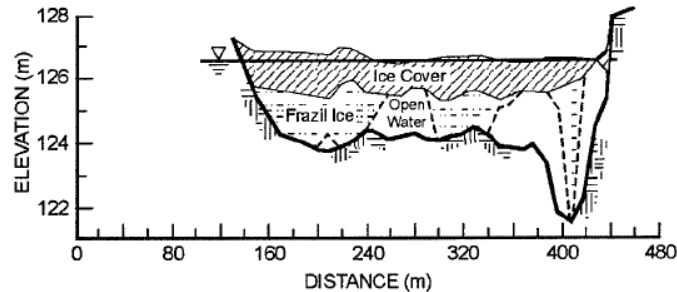


Figure 31 Flow redistribution in a river cross section (adapted from Ettema and Daly, 2004)

Ice cover may also contribute the bed forms. According to Hains and Zabilansky (2004), bed forms tend to be observed under rough ice cover. This might be a factor which needs to be considered to explain the bed forms shown in the multi-beam bathymetry data.

6.2 Could the record St. Clair River ice jam of 1984 cause significant erosion?

It is useful to list some facts about the 1984 ice jam. In April, 1984, the record 24-days ice jam in St. Clair River causes major impact on the water levels and flows. The level of Lake St. Clair dropped about 0.6 m. At the peak of the ice jam, the flow in the St. Clair River was reduced by about 65%. Computer models predicted that the effects on the lake levels should take about one to three years to recover to the pre-jam conditions (Derecki and Quinn, 1986).

At the initial stage of the ice jam, the drifting ice flow downstream to the lower river (delta area) and started to jam. After that, the ice jam progressed upstream rapidly. No record shows whether the ice jam developed upstream to the Lake Huron inlet area. In this report, we assume that the ice jam of 1984 did not.

During the ice jam, large amount of ice floated downstream to the point where the ice movement stopped. Depending on the location, the characteristics of flow and sediment transport are different. The readers are advised to refer to Figure 32 for the definitions of upstream and downstream of the ice jam.

- Upstream of the ice jam, the flow discharge was significantly reduced and the stages were elevated. Globally, sediment upstream of the jam point can not be moved during this period. Sediment particle could move locally due to

mechanisms such as ice grounding, although these effects are deemed as minimal.

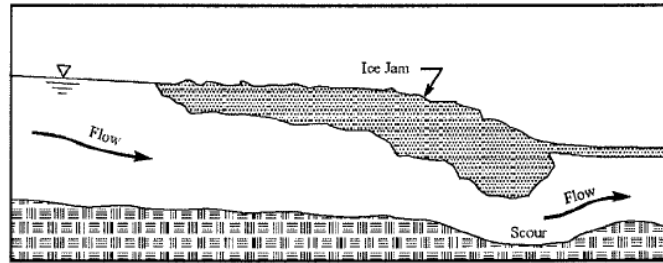


Figure 32. A Schematic view of an ice jam (adapted from Ettema and Daly, 2004)

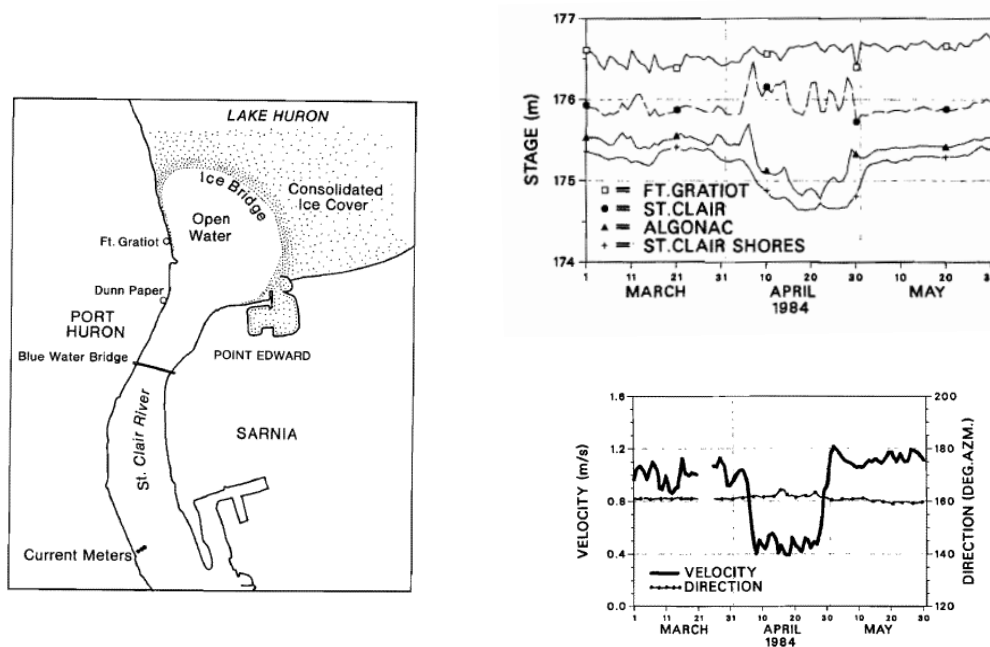


Figure 33. St. Clair River ice jam of 1984: (a) Locations of the ice-bridge and current meters (b) Stages in the river during the ice jam (c) Flow velocity and direction during the ice jam (adapted from Derecki and Quinn, 1986)

- At the ice jam, local scour and deposition could be triggered since at the toe, the ice is thickest and the flow is most restricted. The induced high flow at the toe will cause local scour and deposition the sediment downstream. Recurrent of ice jam in the river may cause substantial scour in the river.
- Downstream of the ice jam, the river is covered with ice over some distance. For this reach of the river, depending on whether the ice cover is fixed or freely floating, the flow and shear stress on the bed is different from open channel flow.
 - If the ice cover is fixed in space, i.e., it can not move up and down, the

river is pressurized (Figure 34). Two controlling parameters here are the pressure head and the roughness of the ice cover (Hains and Zabilansky, 2004). The pressure head is determined by the blocking effect of the ice jam. Higher pressure head means higher flow velocity under the ice cover and higher bed shear stress. For the roughness, experiments have shown that the increase of the ice cover roughness will push the maximum velocity location toward the bed and therefore increase the bed shear stress.

- If the cover is freely floating, than the ice cover roughness is important.

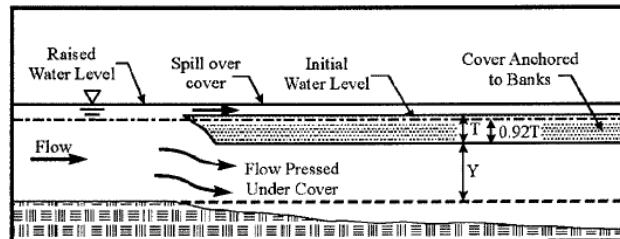


Figure 34. Pressurized flow under an ice cover (adapted from Ettema and Daly, 2004)

After the ice jam breakup, a surge was observed due to the sudden release of water built upstream. The current meter measurement just downstream the first bend shows a surge of flow velocity from about 0.4 m/s to 1.2 m/s as shown in Figure 33. Velocity higher than 1.2 m/s might have occurred somewhere else which was not captured by the current meter. Without the ice jam, the velocity at the measurement location is about 0.8 – 1.0 m/s (from the HydroSed2D simulation and ADCP measurement). We can assume that the sediment transport rate is $q_s \sim \tau_b^{3/2} \sim u^3$, where τ_b is the bed shear stress, u is the velocity magnitude. The surge will cause the sediment transport rate increase 73%-237%.

Since there are very limited measurements during an ice jam event or when the river is covered with ice, the best conclusion we can make is through some rough estimations. We can not conclude with definite answers to the effects of ice on the sediment transport in the St. Clair River. However, the episodic events such as the 1984 ice jam must have played a role which can not be neglected.

6. Navigation Effects

Wuebben et al (1984) has investigated the effects of ship propeller wash, ship waves, and ship drawdown/surges. Some conclusions from Wuebben et al. (1984) are as follows:

- For ship propeller wash, it only gave general guidance by asserting that for most part of the St. Clair River, the ship propeller will suspended the sediment and

- cause scour. No detailed calculation was done.
- For ship drawdown/surges, it claimed that downbound ship, not matter what ship class, will not cause erosion. On the other hand, upbound ship (the worst case is a class 10 vessel traveling upbound), will cause substantial scour for a large portion of the river. Particularly, it specified the portion between St. Clair flats and Stag Island as the most possible erosion area due to ship drawdown/surges.
- For ship waves, it concluded that the worst case for a loaded class 10 vessel traveling upbound with low water level. Base on the 0.5 ft wave height as the critical value for sediment movement, the authors concluded that only the area near the downstream delta slightly exceed this criteria.

In this report, the ship propeller wash is suspected to have contributed to the big hole in the first bend where ships need to maneuver and accelerate/decelerate. Huge surge has been observed by people walking along the river bank near the first bend when a vessel is passing by. This surge of water hit the sheet piles on the bank and spilled over to the road. At that time, wind was not strong. As a rough estimation, Wuebben et al. (1984) calculated the near bed maximum velocity due to the propeller. The efflux velocity may be calculated as

$$V_0 = nD\sqrt{\frac{2K_T D^2}{F}}$$

where n is the propeller revolutions per minute, D is the propeller diameter, K_T is the thrust coefficient (0.25-0.50), F is the area of propeller perpendicular to its horizontal axis. For a 17.5 ft diameter propeller rotating at 90 rpm, V_0 is about 7.32 m/s (24 ft/s). When the water leaves the propeller, it accelerates and then decelerates. The maximum horizontal velocity happens at $V_{x,max}$, where

$$\frac{V_{x,max}}{V_0} = A\left(\frac{X}{D}\right)^a$$

Here X is the horizontal distance from the propeller, a has a value of -0.6 which accounts for the channel bottom effect on the jet, A is a coefficient which depends on the degree of jet limitation. Also assuming that the jet expands at an angle of 13 degree with the horizontal axis, the maximum flow velocity due to the propeller is estimated to be about 5.5 m/s (18 ft/s) for this type of vessel. Although it is hard to calculate the wall shear stress based on this velocity, a comparison is useful. When there is no ship movement, the river has a maximum velocity of about 2 m/s in area of Lake Huron inlet. This velocity corresponds to a maximum shear stress of about 7-8 Pa. Assume a linear relationship between the wall shear and flow velocity (which might not be so accurate), the ship induced wall shear stress will be about 20 Pa. This propeller induced wall shear, together with the ambient bottom shear by the river, is capable of moving sediment size of **64** mm, which is the upper limit of d_{50} of the gravel found in the river.

Another aspect of the navigation effect worth consideration is the so-called downstream-biased sediment transport due to ship propeller (Figure 35). This is due to two reasons. First is that when a vessel is traveling upstream, the thrust needed is more than that of traveling downstream. Higher

bed shear stress will be produced to move the sediment downstream when a vessel heading upstream. The second reason is that on average, when the sediments are entrained and resuspended by the propeller, the river will carry them downstream. These effects might not be so significant by the pass of a single vessel. However, in long term, the cumulative effect shall not be overlooked.

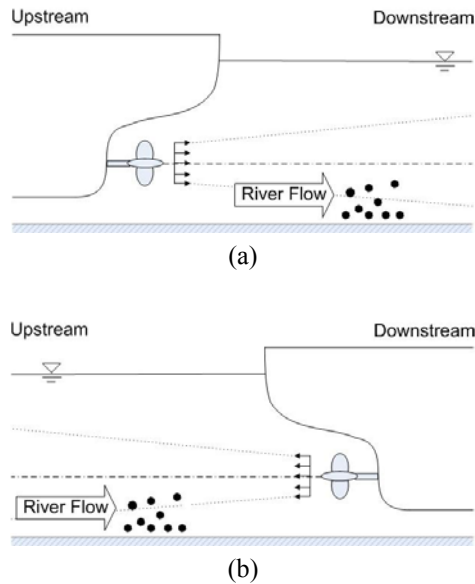


Figure 35. Downstream-biased sediment transport due to ship propeller wash in a river: (a) vessel moving upstream (b) vessel moving downstream

8. Conclusions

HydroSed2D model is carefully calibrated by changing the resistance coefficients in the river. It is also verified by 3D numerical model. Then the HydroSed2D model is used as a tool to study the different aspects of the St. Clair River problem.

Firstly, the calibrated model was used to investigate the factors affecting Lake Huron level. The most important factor is the bathymetry change. From the model results, the river bottom change from 1971 to 2008 contributes about 9-10 cm of Lake Huron level dropping. Simple 1D back water curve calculations also confirm the conclusion regarding the dredging effects for the subcritical St. Clair River. The Lake Huron inlet alignment is found to be not important. The inlet alignment today in the Lake Huron even slightly raises the Lake Huron level.

Secondly, a preliminary shear stress analysis was done to see their implications of sediment transport. The average shear stress in the St. Clair river is about 3-4Pa. It can not move the mean size sediment. Maximum shear stress (~10Pa) is located at the Lake Huron inlet area where scour is possible and the tongue features might be due to that.

Thirdly, a detailed sediment transport and armoring analysis was done by combining HydroSed2D

and the Microsoft Excel tool Acronym. The main conclusion from this analysis confirms the preliminary shear stress analysis and shows that the capacity of the river to move gravel-sized material at all transects is extremely limited. The river should be armored if solely based on the calculation. The lack of imbrication as an evidence of armoring might be explained by causes, such as ship propeller, ice, bioturbation, etc. The local “tongue-like” feature of bed forms at the first two upstream bends does not contradict the global immobility of the gravel. The calculated sediment yield is enough to generate, sustain, and even transform this feature over a period of 10 to 50 years. Long-term morphodynamic simulation of bed evolution along the St. Clair River is not necessary simply because the overall stable status of the river bed.

Lastly, the effects of ice and navigation were reviewed. Ice cover could local redistribute the flow along a cross section and trigger the initiation of bed forms. The record St. Clair River ice jam of 1984 should have caused some scour and deposition locally around the jam. During the ice jam breakup, the sudden release of water caused a surge of flow velocity from about 0.4 m/s to 1.2 m/s. The surge caused the sediment transport rate increase 73% to 237%. Propeller wash induced maximum flow velocity is estimated to be 5.5 m/s which could cause a shear stress of about 20 Pa. This shear stress is capable of moving sediment size of 64 mm, which is the upper limit of d_{50} of the gravel found in the river. A so-called downstream-biased sediment transport due to navigation is hypothesized. Due to the thrust difference between upstream and downstream moving vessels and the preferential downstream movement of the river flow, sediment movement due to navigation is downstream-biased. The cumulative effect of this downstream-biased sediment movement over a long time period might be significant.

Appendix A

In this appendix, the armoring analysis results for all transects are listed.

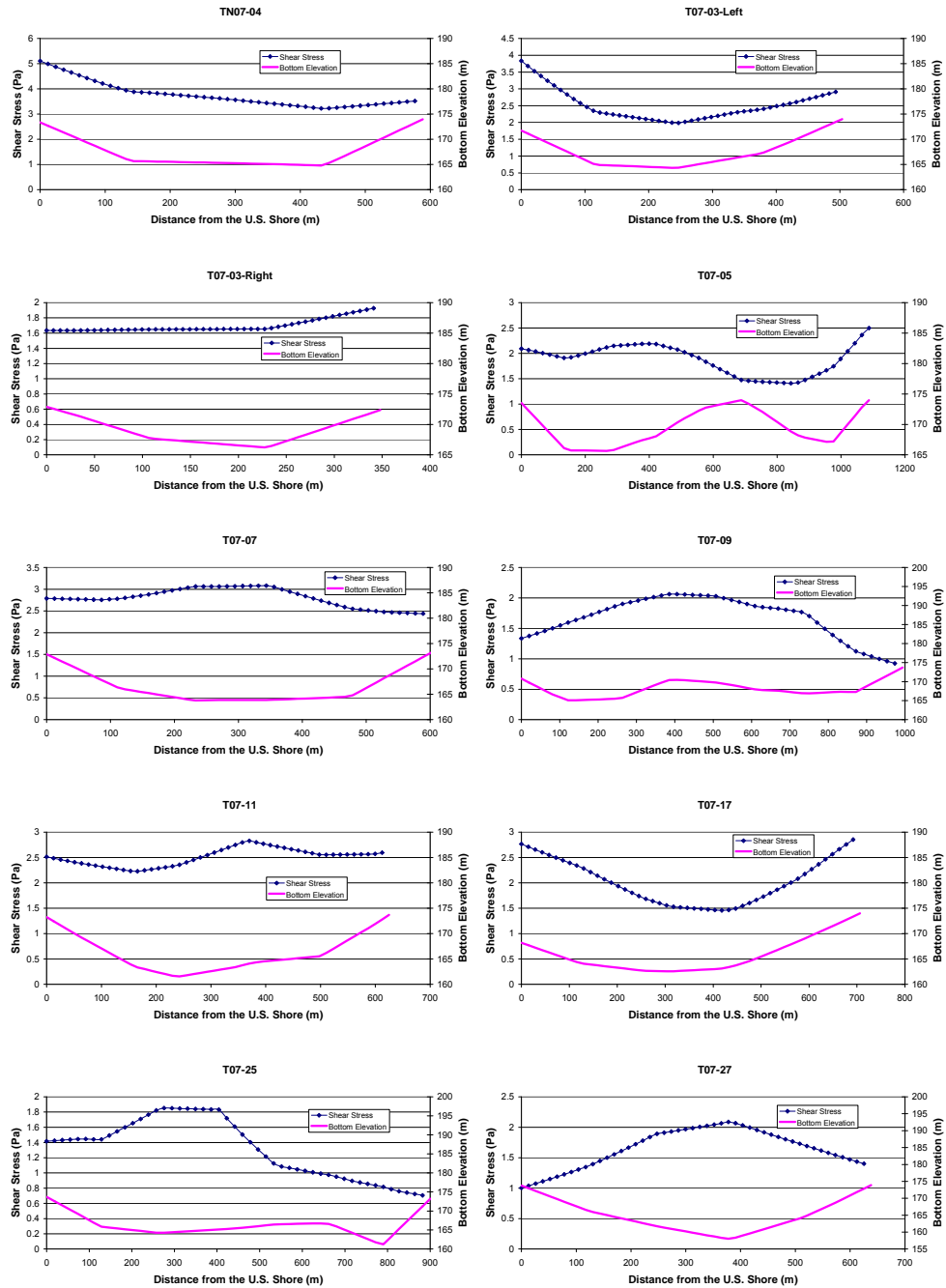


Figure 36. Shear Stress Distributions along the Transects Analyzed for the St. Clair River for Discharge of $5410 \text{ m}^3/\text{s}$ (Corresponding to 50% on the Flow Duration Curve)

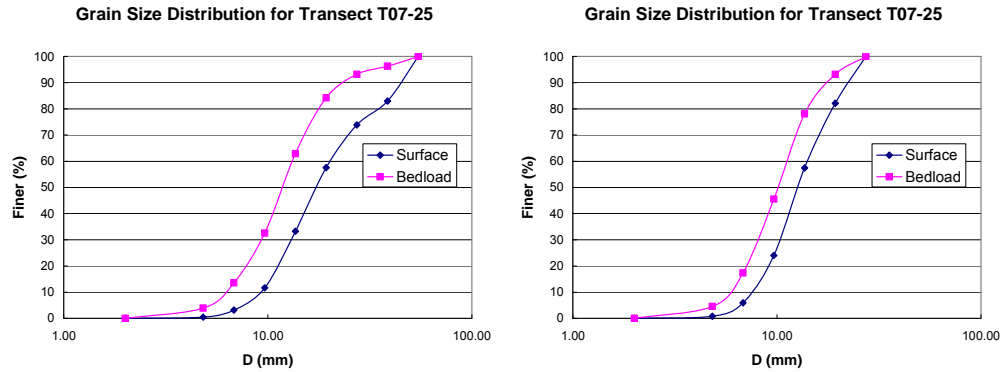


Figure 37. Surface and Bedload Sediment Size Distributions for the Transects along the St. Clair River

References

Baird & Associates (2005). *Regime change (man made intervention) and ongoing erosion in the St. Clair River and impacts on Lake Michigan-Huron lake levels*. Technical report, W.F. Baird & Associates Coastal Engineering Ltd., Oakville, Ontario, June 2005.

G. Parker (1990). Surface-based bedload transport relation for gravel rivers. *Journal of Hydraulic Research*, 28(4):417–436, 1990.

X. Liu and M.H. García (2008a). A 3D numerical model with free water surface and mesh deformation for local sediment scour. *Journal of Waterway, Port, Coastal, and Ocean Engineering*. 134(4): 203-217.

X. Liu and M.H. García (2008b). Two-dimensional scour simulations based on coupled model of shallow water equations and sediment transport on unstructured meshes. *Coastal Engineering*, 55(10):800-810.

X. Liu (2008c). Numerical models for scour and liquefaction around object under currents and waves. PhD thesis, University of Illinois at Urbana and Champaign, 2008.

X. Liu and M.H. García (2007), Numerical Modeling of the Calumet Water Reclamation Plant (CWRP) Primary Settling Tanks, Civil Engineering Studies, Hydraulic Engineering Series No 80, Department of Civil and Environmental Engineering, University of Illinois at Urbana-Champaign.

G. H. Keulegan, 1938, Laws of turbulent flow in open channels, National Bureau of Standards Research Paper RP 1151, USA.

OpenCFD (2008), OpenFOAM: The open source computational fluid dynamics (CFD) toolbox. <http://www.OpenFoam.org> (Nov. 10, 2008).

V.T. Chow (1959), Open-channel Hydraulics, McGraw-Hill Book Company.

J.L. Wuebben, W.M. Brown, and L.J. Zabilansky, 1984, Analysis of Physical Effects of Commercial Vessel Passage through the Great Lakes Connecting Channels, Contract to the Detroit District, U.S. Army Corps of Engineers by the USA Cold Regions Research and Engineering Laboratory, Internal Report 884.

B. Dargahi (2003). Three-dimensional modeling of ship-induced flow and erosion. *Proceedings of the Institution of Civil Engineers, Water & maritime Engineering*, 156(WM2):193-204.

J.A. Derecki (1985). Effect of channel changes in the St. Clair River during the present century. *Journal of Great Lakes Research*, 11(3):201-207.

J.A. Derecki and F.H. Quinn (1986), Record St. Clair River Ice Jam of 1984. *Journal of Hydraulic Engineering*, 112(12): 1182-1194.

R. Ettema and S.F. Daly (2004), Sediment transport under ice, USA Cold Regions Research and Engineering Laboratory, U.S. Army Corps of Engineers, Report number ERDC/CRREL TR-04-20.

G.D. Ashton (1986), River and Lake Ice Engineering, Water Resources Publication.

D. Hains and L. Zabilansky (2004), Laboratory test of scour under ice: data and preliminary results, USA Cold Regions Research and Engineering Laboratory, U.S. Army Corps of Engineers, Report number ERDC/CRREL TR-04-9.

M.H. García (2006), Sedimentation Engineering: Processes, Measurements, Modeling, and Practice, ASCE Manuals and Reports on Engineering Practice No. 110, published by the American Society of Civil Engineers.

Nitrate Remeidation by Iron Redox Reactions in Soils

Basic Information

Title:	Nitrate Remeidation by Iron Redox Reactions in Soils
Project Number:	2009IL171B
Start Date:	5/1/2009
End Date:	4/30/2010
Funding Source:	104B
Congressional District:	15
Research Category:	Water Quality
Focus Category:	Nitrate Contamination, Water Quality, Treatment
Descriptors:	None
Principal Investigators:	Joseph Stucki, Zachary B. Day, Fabian G. Fernandez

Publications

There are no publications.

Abiotic Nitrate Reduction by Redox Activated Iron-Bearing Smectites

PI: Professor Joseph W. Stucki

Department of Natural Resources and Environmental Sciences, University of Illinois, Urbana-Champaign
1102 South Goodwin Avenue
Urbana, Illinois 61801
jstucki@illinois.edu
(217) 333-9636

PROBLEM AND RESEARCH OBJECTIVE

Nitrate is an important inorganic nitrogen species, key to the healthy growth of all vegetation either through direct uptake or indirectly through processes involving a range of bacteria within the soil and root systems. Logically, this makes nitrate a target of most fertilizer regimens, with tons applied annually to fields in most all agricultural regions. Combined with irrigation, rain, natural water tables and nitrate's high solubility, its widespread contamination of water sources in human populated areas is not surprising.

A litany of negative human health effects are attributed to these high levels of nitrate, including an increased risk of a number of cancers, chronic diseases and birth defects (Camargo and Alonso, 2006). Nitrate also contributes extensively to the acidification of, eutrophication of, and hypoxia in bodies of water in nearly every coastal region with significant human population. Hypoxia is especially of major concern in the Gulf of Mexico, particularly near the Mississippi River delta (Camargo and Alonso, 2006; Hypoxia Action Plan, 2007). Beyond the direct health and environmental stresses caused by nitrate, economic side effects can be felt in the strains on health care these issues pose and the loss of income in areas reliant on clean waters for fishing and tourism.

Additionally, clean up and immobilization efforts at sites dealing with contamination by oxidation-reduction (redox) active heavy metals (e.g. cobalt, technetium, and uranium) are hampered by the high levels of nitrate that are also present. Nitrate, sitting higher in the reduction series, must be dealt with first before any method of sequestration relying on redox reactions within the organic, inorganic, or both portions of the soil is attempted. To this end, understanding the interactions between nitrate with the redox active, iron containing portions of soils is necessary.

Most studies of nitrate and the nitrogen cycle within soils have focused primarily on bacterial processes. Some studies, however, have investigated abiotic nitrate reduction which have focused primarily on two aspects. The first is on a class of compounds known as green rusts (layered Fe(II)Fe(III) hydroxide, GR) which have been shown in the laboratory to be an excellent reductant of nitrate. While thought to exist in soils, they have yet to be characterized *in situ* due to their highly oxygen sensitive nature (Hansen *et al.*, 1994, 1996, 1998, 2001). Studies by numerous groups have also shown zero-valent iron to be an excellent reductant of nitrate (Miehr *et al.*, 2004; Alowitz *et al.*, 2002; Sianta *et al.*, 1996; Till *et al.*, 1998; Huang *et al.*, 1998; Devlin *et al.*, 2000; Westerhoff, 2003; Sohn *et al.*, 2006).

A third, but little studied avenue of nitrate abiotic nitrate reduction was proposed by Ernstsén (Ernstsén, 1996; Ernstsén *et al.*, 1998) who observed a sharp, dramatic decrease in nitrate levels within Danish soil profiles. Denitrifying bacteria were absent from these soils, demonstrating the existence of some type of abiotic pathway leading to nitrate reduction. She proposed that Fe(II) within the structure of the soil clay minerals that was responsible for this reduction. The structural Fe(II) was produced by iron-reducing bacteria within the soil. Because Ernstsén's hypothesis concerning redox active soil clay minerals interacting with nitrate has

received no further study but significant merit for a more detailed investigation, the present study was undertaken to determine whether such a phenomenon can be demonstrated in the laboratory.

METHODOLOGY

Sample Preparation and Reduction

All experiments were performed using the Source Clays Repository recognized ferruginous smectite, SWa-1—hereafter referred to as “SWa-1” and “clay” within the methods section for ease of reading. All water used is first purified by a Barnstead Fisher NanoPure System Model D4741, fed by a DI water source.

Each experiment described was performed in triplicate, with each reaction in a separate 50 mL polycarbonate centrifuge tube. The centrifuge tubes were sealed with an air-tight septum cap and all manipulation were performed under inert-atmosphere conditions, using needles to access the sample suspensions through the septum before or after centrifugation (Stucki *et al*, 1984).

Each sample tube received a fresh preparation of citrate-bicarbonate (C-B) buffer from stock solutions for each trial. The buffer components were 5 mL 0.18 M sodium citrate (Fisher Scientific, Waltham, Massachusetts) in water, 10 mL 0.36 M sodium bicarbonate (Fisher Scientific, Waltham, Massachusetts) in water, and an additional 15 mL of water. Final buffer concentrations were 0.03 M sodium citrate and 0.12 M sodium bicarbonate in a 30 mL total volume. Into each tube was then weighed a 50 mg sample of SWa-1. Tubes were capped and mechanically vortexed for 20 min, suspending their contents.

Tube contents were chemically reduced using sodium dithionite (Mallinckrodt Baker, Lopatcong Township, New Jersey) as described by Stucki et al (1984). A 200 mg portion of sodium dithionite was weighed and added to the C-B clay suspension in each reaction tube, after which the tube was immediately septum sealed and placed in a 70 °C water bath. Two needles were inserted through the septum cap. One needle brought nitrogen gas, which previously passed through an oxygen trap, into the tube; the second needle vented excess gas, purging gaseous reaction products (e.g. H₂S) from the system. Because the mass of reductant added to each reaction was constant, the extent of reduction was controlled by reaction time within the water bath. Reactions were quenched by submersion of the tubes into liquid nitrogen. Experimental runs were defined by these reduction times as follows: 10 min, 30 min, 60 min, 240 min and an unaltered control group that was not reduced.

After quenching the reaction in liquid nitrogen, tubes were centrifuged at 19000 rpm (18000 x g) for 20 min in a Sorvall RC 50 Plus centrifuge. Tube contents were washed three times with deoxygenated 5 mM NaCl solution in water. The clay mixtures were resuspended by vortexing between washes. A fourth, final wash was performed with 18 MOhm-cm pure water before analyses for iron oxidation state and/or before reaction with nitrate.

Iron Analysis

The washed clay with little remaining supernatant was analyzed for Fe(II) and total Fe content using a 1,10-phenanthroline and UV light method, modified slightly from Komadel and Stucki (1988). Method modification required digestion of samples and standards in polycarbonate centrifuge tubes instead of polypropylene tubes to avoid sample transfer resulting in loss and reoxidation. Analysis batches averaged between three and six washed clay samples,

representing one or two different reduction time trials, as well as four standards to verify the accuracy of the analysis.

Each standard was prepared in a polycarbonate centrifuge tube identical to the reduction reaction tubes. Tubes were labeled according to their approximate iron concentrations after final dilution as 0, 1, 3, and 5 ppm. The mass of each empty tube was recorded and into each approximately 7 mg of ferrous ammonium sulfate (Allied Chemical and Dye, New York, New York) was weighed per integer of final desired concentration in ppm. The weight of the tube and the standard were recorded so exact concentration could be determined calculated. After adding the standard to the tube, all white lights in the room where the analysis was being performed were turned off in favor of red lights. This prevented ferric iron in samples, which also forms a complex with 1,10-phenanthroline, from being photo-chemically reduced before Fe(II) concentrations had been determined.

Digestion and complexing reagents were added in fast succession to each standard and sample to prevent as much reoxidation of the reduced clay samples in the presence of air as possible; reduced clay samples were only uncapped just before addition of digestion reagents. A 12.0 mL aliquot of 3.6 N sulfuric acid produced from concentrated sulfuric acid (Mallinckrodt Baker, Lopatcong Township, New Jersey), a 2.0 mL aliquot of 10% by weight 1,10-phenanthroline (Sigma-Aldrich, St. Louis, Missouri) in 95% ethanol, and 1.0 mL of 49% hydrofluoric acid in water (Acros Organics, Geel, Belgium) were added to all standards and samples. The centrifuge tubes were placed in a boiling water bath for 30 min to digest their contents, followed afterwards by a 15 minute cooling period. Once cooled, 10.0 mL of 5% by weight boric acid (Acros Organics, Geel, Belgium) in water was added to each centrifuge tube.

Centrifuge tube contents were quantitatively transferred to 100 mL polypropylene tubes, which had previously been weighed while empty. Each of these “iron analysis tubes” was filled to within an inch of its tops with water and its final mass recorded. Mass was converted to volume assuming a density of 1.000 g/ml. A piece of parafilm was placed securely across the top of each tube to prevent spilling and the tube was then inverted several times to induce mixing. After mixing, a Brinkmann Dosimat dilutor was used to draw a 2.0 mL aliquot from the tube and to expel it into a 50-mL Erlenmeyer flask along with 20.0 mL of 1% by weight sodium citrate solution in water. Two such flasks were produced from each iron analysis tube for duplicate absorbance measurement.

Final solutions were analyzed on a Varian Cary 5 UV-Vis spectrophotometer equipped with a Routine Sampling Accessory (RSA) Internal Sipper using the Concentration software application provided by Varian. The spectrometer was allowed to warm up for a minimum of 30 min prior to zeroing and sample analysis. The absorbance of the tris-(1,10-phenanthroline)Fe(II)²⁺ complex was measured at 510 nm, with two replicate measurements taken from each flask. During Fe(II) analysis the room was illuminated with only subdued red light, and the sipper line was rinsed twice with water between samples to prevent cross contamination. After absorbance values were collected for Fe(II), all flasks were placed in an enclosure with two high intensity mercury vapor lamps for 2 h to reduce the ferric iron complex with 1,10-phenanthroline (Stucki and Anderson, 1981). The total Fe absorbance values were then measured at 510 nm.

Nitrate Addition

A second group of reduced, washed clay samples from each reduction-time set were identically prepared to be reacted with nitrate. An 88 μM solution of sodium nitrate (EM Science, Gibbstown, New Jersey) was prepared in water. For each sample a 20.0 mL aliquot of nitrate was prepared in a capped centrifuge tube. Each was deoxygenated by flowing nitrogen into the solution for a minimum of 30 min through a needle which penetrated the septum cap, venting excess gas through a second needle. Nitrogen flow was continued while the aliquot was drawn from the centrifuge tube by a gas tight syringe and injected into a tube containing the washed, reduced clay, also equipped with nitrogen supply and vent needles.

After injection, the clay was suspended in the nitrate solution by mechanical vortex and then tubes were placed on a shaker plate for 18 h. Samples were centrifuged and affixed with a nitrogen needle and vent needle in the headspace, so as not to disturb the supernatant liquid or the collected solid at the bottom. The supernatant was carefully removed by gas tight syringe and placed in a new tube which was then frozen for shipping to be analyzed for NO_x^- and nitrite as described below. The remaining clay was analyzed by the 1,10-phenanthroline method for iron content to compare with samples not reacted with nitrate.

A control group for the 10-min, 30-min, 60-min, and 240-min reduction time trials was created as well. These samples were reduced and treated exactly as those that were treated with nitrate up to the point of nitrate addition. Instead of a dilute nitrate solution, these samples were treated with 20 mL each of deoxygenated water for 18 h. As no nitrate was present, supernatants were not analyzed for nitrogen. This control experiment was performed to account for any reoxidation of the clay structure not attributed to nitrate.

Nitrogen Speciation Analysis

Nitrite and nitrate were analyzed together using a modification of the method described by Braman and Hendrix (1989) to determine NO_x^- concentrations using a Thermo Model 42i Chemiluminescence Analyzer. The sample holder on the instrument was filled with 100 mL of acidified (1-2 M HCl) 0.10 M V(III) solution, bubbled with helium. Instrument response was calibrated by 100 μL injections of NO_x^- standards ranging in concentration from 1 to 50 μM . Evolved NO was carried by helium flow to the analyzer and the peak area recorded. Sample injection volume was varied between 50 and 200 μL .

Nitrite alone was measured using a modified Garside (1982) method. The method was modified such that it was identical to the combined nitrite and nitrate method described above with the exception of the reagent solution in the sample holder. The nitrite only mixture was a 1:3:6 ratio of 3% w/v sodium iodide in water, glacial acetic acid, and pure water. Calibration and sample analysis were carried out as above.

Results

Iron Analysis

Following each iron analysis trial, absorbance values for the standards were plotted against their known iron concentrations to create calibration curves. Curves were used to verify both that the method returned a linear response within the concentration range and that the specific trial set was responding properly. Calibration curves constructed for both Fe(II) and total Fe for a single trial run were uniformly linear with correlation coefficients within the same range as those in the figures, excepting one trial with one outlying standard.

Accuracy and precision were also correlated across the entire experimental range using the Beer-Lambert Law

$$A = \varepsilon \cdot c \cdot l \quad (1)$$

where A is the absorption value, ε is the absorptivity coefficient in $\text{M}^{-1}\text{cm}^{-1}$, c is the molar concentration and l is the path length (1 cm) of the cell used. Using the known concentrations of the standards analyzed in each trial in conjunction with the absorption values obtained, the absorptivity of all standards was calculated. The absorptivity values were averaged, excluding the single outlier, resulting in absorptivity coefficients of $931 \text{ M}^{-1}\text{cm}^{-1} \pm 5\%$ for Fe(II) and $1044 \text{ M}^{-1}\text{cm}^{-1} \pm 4\%$ for total Fe. The slightly higher value of the total Fe absorptivity coefficient versus that of Fe(II) is in agreement with the findings of Komadel and Stucki (1988).

Using the absorptivity coefficients derived from the standards, the Beer-Lambert law was again used to calculate the concentrations of Fe(II) and total Fe present in the sample solutions. The concentrations were normalized by dividing by the mass of clay used in each trial, and then these values are averaged across each time set and a ratio between Fe(II) and total Fe was derived (Table 1).

The “unaltered” samples—those that were unreacted with dithionite—showed only a trace amount of Fe(II) which is negligible compared to the total Fe content. The amount of Fe(II) present in the unaltered samples is the same both before and after reaction with a dilute nitrate solution. The remaining sample sets in the before nitrate reaction group have consistent total Fe concentrations. The total Fe values after reaction with nitrate are likewise consistent within themselves, but show a slight decrease, likely due to dissolution in the unbuffered nitrate solution.

After only 10 min of reduction in the presence of dithionite, the Fe(II) content increased dramatically accounting for roughly a quarter of the total Fe in the structure. Following reaction with nitrate, the Fe(II) content of the 10-min trials, however, failed to drop significantly.

Interestingly, the extent of reduction in the 30-minute 60-min samples was similar, with both falling in the 50-60% range. The values after introduction to nitrate were likewise similar to each other, but a large amount of reoxidation was evident in both cases. After 420 min of reduction, nearly all ferric iron in the clay structure was converted to Fe(II). Comparing all the values obtained for all time trials revealed that a large amount of reduction occurred in approximately the first 30 min of reaction and the rate of the reaction significantly decreased after that point. The Fe(II) to total Fe ratios in 10-, 30- and 60-min control trials, in which reduced clay was exposed only to water, were not significantly different from those of the clay directly after reduction; so most of the reoxidation occurring was attributed to the redox reaction with nitrate.

The 240-min samples exhibited the most reoxidation in the presence of nitrate. Note, however, that the 240-min samples were not reoxidized to the same extent as the 30-min and 60-min samples, which in turn were not as reoxidized as the 10-min samples. This suggests that the structural Fe(II) is not all available to be reacted with nitrate. This may in large part be due to the random reduction of Fe sites at the basal surface. The nitrate anion is unlikely to react at the basal surfaces due to coulombic repulsion. Reaction then only occurs at the comparatively small surface area of the edge sites (approximately 0.1% of clay surface area), which contain a small percentage of the total Fe(II) within the structure, as illustrated by Ribeiro *et al.* (2009). If so, some form of electron transfer to the edge sites is necessary for the complete reoxidation of the clay structure. The 240-min samples were the only group that exhibited significant reoxidation in water, with the structural Fe(II) to total Fe ratio some 20% lower than in the clay after being reduced.

Nitrogen Speciation

The nitrogen speciation for the reduced clay samples (Table 2) revealed that the general trend is for NO_x^- values to decrease from their original 88 μM concentration as the extent of reduction in the clay increases. An unexpected slight decrease in NO_x^- concentration within the unaltered samples, comparable to that in the 10-min samples, suggests a slight error in the method of approximately $\pm 1.5 \mu\text{M}$. No nitrite appears in the solutions of the unaltered samples, confirming that no nitrate was likely lost from the unaltered samples. Nitrite concentrations among all reduced samples were extremely low and comparable with one another. Nitrite, therefore, was not a major reduction product in these reactions: far more NO_x^- was lost relative to how much of the remaining NO_x^- was nitrite. Furthermore, nitrite concentrations failed to increase with increasing extent of reduction or with total nitrate reduced (Table 3). Nitrate remaining was calculated as nitrite values subtracted from NO_x^- and total nitrate reduced is the calculated nitrate concentration subtracted from the initial concentration in the nitrate solution used of 88 μM multiplied by the volume of the aliquot introduced to the sample (20 mL).

Looking at the nitrogen speciation and iron analysis together as a whole, chemically reduced clay clearly was very much capable of nitrate reduction, as hypothesized. By plotting the amount of Fe(II) initially available vs. the amount of nitrate reduced (Figure 1), a clear trend between the extent of reduction within the clay structure and the amount of reduced nitrate is visible. The points do not fall all exactly upon a line, because, as noted previously, the state of reduction within the structure was such that variable amounts of Fe(II) are available at the edge given the same overall amount of reduction of the structure.

PRINCIPAL FINDINGS AND SIGNIFICANCE

The data presented show that nitrate is abiotically reduced by chemically reduced clays, which concomitantly are oxidized in the process, thus removing removing the nitrate from the system. A clear relationship was drawn between the amount of Fe(II) present in the clay structure and the amount of nitrate that is removed from a dilute solution. The reactive sites evidently are located on the edge surfaces of the clay layers, which present much less reactive surface area than the basal surfaces. Not explored in these experiments was the effect of different clays upon the reactions. SWa-1 was selected for this pilot study because it is known to have one of the highest rates of iron substitution in the octahedral sheet. It stands to reason that clays containing less octahedral iron, containing tetrahedral iron, and those with a different layer structure (1:1, 2:1:1) will behave differently. Since a smectite such as SWa-1 is not representative of the minerals found at all sites requiring nitrate remediation, it must be ascertained whether or not other phyllosilicates have similar reactivity. As well, the kinetics of these reactions are not understood. The methods used in the experiments described here could easily be altered to assess the amount of reoxidation and nitrate removal at intervals other than 18 h.

While the findings of these experiments were all based upon chemical reduction, it seems logical that bacteria reduced clays found in natural settings would be capable of the same reaction. This is especially true in light of the fact that bacteria reduced clays have been shown to have their Fe(II) concentrated at edge sites, which is conducive to the proposed mechanism for reduction of nitrate by the reduced clay minerals. Further experiments using various clays in addition to SWa-1, as detailed above, may confirm or disconfirm this hypothesis.

There is still a great deal more to be explored concerning reduced mineral interactions with nitrate. With any luck, the literature will eventually be as detailed for this set of reactions as for nitrate's interactions with green rust and with zero-valent iron.

NOTABLE ACHIEVEMENTS

This study has increased scientific understanding, providing evidence that redox active, iron-bearing clay phases within soils are capable of, and may play a key role in, nitrate reduction. The 1,10-phenanthroline iron analysis method was also slightly improved to allow analysis of wet and oxygen sensitive samples without initial transfer and loss to new analysis tubes.

STUDENT SUPPORTED WITH FUNDING

Zachary B. Day, Department of Natural Resources and Environmental Sciences, University of Illinois at Urbana-Champaign, Master of Science, May 2010.

PUBLICATIONS AND PRESENTATIONS

- Alowitz, M.J., Scherer, M.M. (2002) Kinetics of nitrate, nitrite, and Cr(VI) reduction by iron metal. *Environmental Science and Technology*, **36**, 299-306.
- Braman, R.S. & Hendrix, S.A. (1989) Nanogram Nitrite and Nitrate Determination in Environmental and Biological Materials by Vanadium(III) Reduction with Chemiluminescence Detection. *Analytical Chemistry*, **61**, 2715-2718.
- Camargo, J.A. & Alonso, Á. (2006) Ecological and toxicological effects of inorganic nitrogen pollution in aquatic ecosystems: A global assessment. *Environment International*, **32**, 831-849.
- Devlin, J.F., Eedy, R.; Butler, B.J. (2000) Effect of electron donor and granular iron on nitrate transformation rates in sediments from a municipal water supply aquifer. *Journal of Contaminant Hydrology*, **46**, 81-97.

- Ernstsen, V. (1996) Reduction of Nitrate by Fe²⁺ in Clay Minerals. *Clays and Clay Minerals*, **44**, 599-608
- Ernstsen, V., Gates, W.P., Stucki J.W. (1998) Microbial reduction of structural iron in clays A renewable source of reduction capacity. *Journal of Environmental Quality*, **27**, 761–766.
- Garside, C. (1982) A chemiluminescent technique for the determination of nanomolar concentrations of nitrate and nitrite in seawater. *Marine Chemistry*, **11**, 159-167.
- Hansen, H.C.B. and Koch, C.B. (1998) Reduction of nitrate to ammonium by sulphate green rust: Activation energy and reaction mechanism. *Clay Minerals*, **33**, 87-101
- Hansen, H.C.B., Borggaard, O.K., Sorensen, J. (1994) Evaluation of the free energy of formation of Fe(II)-Fe(III) hydroxide-sulphate (green rust) and its reduction of nitrite. *Geochimica et Cosmochimica Acta*, **58**, 2599-2608
- Hansen, H.C.B., Koch, C.B., Nanckekrogh, H., Borggaard, O.K., Sorensen, J. (1996) Abiotic nitrate reduction to ammonium: Key role of green rust. *Environmental Science and Technology*, **30**, 2053-2056.
- Hansen, H.C.B., Guldberg, S., Erbs, M., Koch, C.B. (2001) Kinetics of nitrate reduction by green rusts - Effects of interlayer anion and Fe(II):Fe(III) ratio. *Applied Clay Science*, **18**, 81-91.
- Huang, C.P., Wang, H.W., Chiu, P.C. (1998) Nitrate reduction by metallic iron. *Water Resources*, **32**, 2257-2264.
- Komadel, P. & Stucki, J.W. (1988) Quantitative assay of minerals for Fe²⁺ and Fe³⁺ using 1,10-phenanthroline: III. A rapid photochemical method. *Clays and Clay Minerals*, **36**, 379-381.

- Miehr, R., Tratnyek, M.M., Bandstra, J.Z., Scherer, M.M., Alowitz, M.J., Bylaska, E.J. (2004) Diversity of contaminant reduction reactions by zerovalent iron: role of the reductate. *Environmental Science and Technology*, **38**, 139-147.
- Mississippi River/Gulf of Mexico Watershed Nutrient Task Force (2007) Draft Gulf Hypoxia 2008 Action Plan
- Ribeiro, F.R., Fabris, J.D., Kostka, J.E., Komadel, P., Stucki, J.W. (2009) Comparisons of structural iron reduction in smectites by bacteria and dithionite: II. A variable-temperature Mossbauer spectroscopic study of Garfield notronite. *Pure and Applied Chemistry*, **81**, 1499-1509.
- Sohn, K., Kang, S.W., Ahn, S., Woo, M., Yang, S.K. (2006) Fe(0) nanoparticles for nitrate reduction: Stability, reactivity, and transformation. *Environmental Science and Technology*, **40**, 5514-5519.
- Sianta, D.P., Schreier, C.G., Chou, C.S., Reinhard, M. (1996) Treatment of 1,2-dibromo-3-chloropropane and nitrate-contaminated water with zerovalent iron or hydrogen/palladium catalysts. *Water Resources*, **30**, 2315-2322.
- Stucki, J.W. and Anderson, W.L. (1981) The quantitative assay of minerals for Fe²⁺ and Fe³⁺ using 1,10-phenanthroline. I. sources of variability. *Soil Science Society of America Journal*, **45**, 633-637.
- Stucki, J.W., Golden, D.C., Roth, C.B. (1984) Preparation and handling of dithionite-reduced smectite suspensions. *Clays and Clay Minerals*, **32**, 191-197.
- Till, B.A., Weathers, L.I., Alvarez, P.J.J. (1998) Fe(0)-supported autotrophic denitrification. *Environmental Science and Technology*, **32**, 634-639.

Westerhoff, P. (2003) Reduction of nitrate, bromate and chlorate by zero valent iron (Fe0).

Journal of Environmental Engineering, **129**, 10-16.

TABLES

Table 1. Iron Analysis Results

		Reduction Time (min)				
		0*	10	30	60	240
Before Nitrate Treatment	mmol Fe(II) / g Clay	0.01	0.42	0.98	0.88	1.76
	mmol Fe / g Clay	2.68	1.63	1.63	1.69	1.98
	Fe(II)/Fe	0.00	0.25	0.60	0.52	0.89
After Nitrate Treatment	mmol Fe(II) / g Clay	0.01	0.33	0.47	0.61	0.74
	mmol Fe / g Clay	1.49	1.53	1.43	1.56	1.43
	Fe(II)/Fe	0.01	0.21	0.33	0.39	0.52
After Water Treatment	mmol Fe(II) / g Clay	n.d.	0.43	0.80	0.80	0.89
	mmol Fe / g Clay	n.d.	1.47	1.46	1.26	1.25
	Fe(II)/Fe	n.d.	0.28	0.55	0.64	0.70

*Unaltered Sample

Table 2. Nitrogen Speciation Results

Sample	[NO _x ⁻] (μM)	[NO ₂ ⁻] (μM)
Unaltered	86.7	0.0
10-min	87.0	0.1
30-min	84.7	0.1
60-min	83.4	0.2
240-min	83.0	0.1

Table 3. Nitrate Reduced

Reduction Time	[NO ₃ ⁻] Remaining (mM)	[NO ₂ ⁻] Present (mM)	NO ₃ ⁻ Reduced (mmol)
Unaltered	0.0867	0.0000	2.6 x 10 ⁻⁵
10 min	0.0870	0.0002	2.2 x 10 ⁻⁵
30 min	0.0848	0.0001	6.6 x 10 ⁻⁵
60 min	0.0834	0.0002	9.6 x 10 ⁻⁵
240 min	0.0830	0.0001	1.02 x 10 ⁻⁴

FIGURES

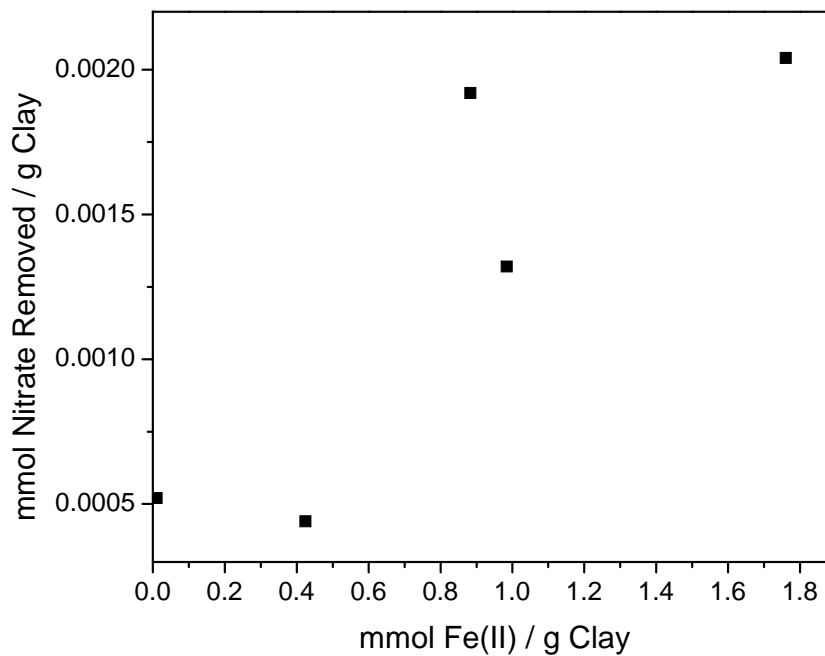


Figure 1. Plot showing the effect of the extent of reduction of a clay mineral on the amount of nitrate reduced.

Attachement and Transport Mechanisms of Cryptosporidium parvum Oocysts in Subsurface Environments: A Multi-Scale Study

Basic Information

Title:	Attachement and Transport Mechanisms of Cryptosporidium parvum Oocysts in Subsurface Environments: A Multi-Scale Study
Project Number:	2009IL173B
Start Date:	5/1/2009
End Date:	8/14/2010
Funding Source:	104B
Congressional District:	15
Research Category:	Ground-water Flow and Transport
Focus Category:	Water Quantity, Groundwater, Agriculture
Descriptors:	
Principal Investigators:	Helen Nguyen, Yuanyuan Liu

Publications

There are no publications.

Project Title: Attachment and transport mechanism of *Cryptosporidium parvum* oocysts in subsurface environments: a multi-scale study

Project Type: Research

Focus Categories: water quality, groundwater, agriculture

Research Category: Groundwater Flow and Transport, Water Quality, Biological Sciences, Engineering

Keywords: pathogen transport, groundwater contamination, manure

Start Date: August 15, 2009

End Date: August 14, 2010.

Principal investigator: Helen Nguyen
Assistant Professor
Department of Civil and Environmental Engineering
University of Illinois at Urbana-Champaign
205 N.Mathews
3230 Newmark Lab, MC 250
Urbana IL 61801
Phone 217-244-5965
Fax 217-333-6968
webpage <http://cee.uiuc.edu/Faculty/nguyen.htm>

Congressional District of the university where the work is to be conducted: 15

1. Research Objective

Pathogens including *Cryptosporidium parvum* oocysts found in surface runoff are one of the leading causes of impaired river and estuary water. Knowledge on the fate and transport of *C. parvum* oocysts in agricultural runoff is currently lacking and is urgently needed to protect water supplies for many parts of the state. The results of this project will provide a scientific basis for water resources and environmental *sustainability*.

This project uses a **multi-scale approach** to identify *chemical and physical factors* that influence attachment and mobility of *C. parvum* oocysts. A comprehensive understanding of these factors will be used to develop a model to predict the fate and transport of oocysts in the subsurface environment. The **objectives** of this project are: (1) to investigate the role of oocyst wall macromolecules in the deposition and transport of *C. parvum* oocysts by systematically modifying the oocyst wall; (2) to determine the attachment mechanisms of *C. parvum* oocysts on inorganic (i.e. quartz) and organic (i.e. coated with natural organic matter) soil surfaces on a microscopic scale; and (3) to determine the transport of *C. parvum* oocysts in the subsurface environment in micromodel setups. The experimental approach ranges from a **microscopic to a macroscopic scale**. A novel microscopic technique consisting of a radial stagnation point flow (RSPF) cell combined with a microscope will be used to monitor attachment and detachment kinetics of oocysts under well-defined flow conditions in real time. Deposition and detachment experiments will be conducted with systematically varied solution conditions to determine the mechanisms of oocyst interaction with representative soil surfaces. Pore scale transport of oocysts will be studied using a precisely fabricated micromodel.

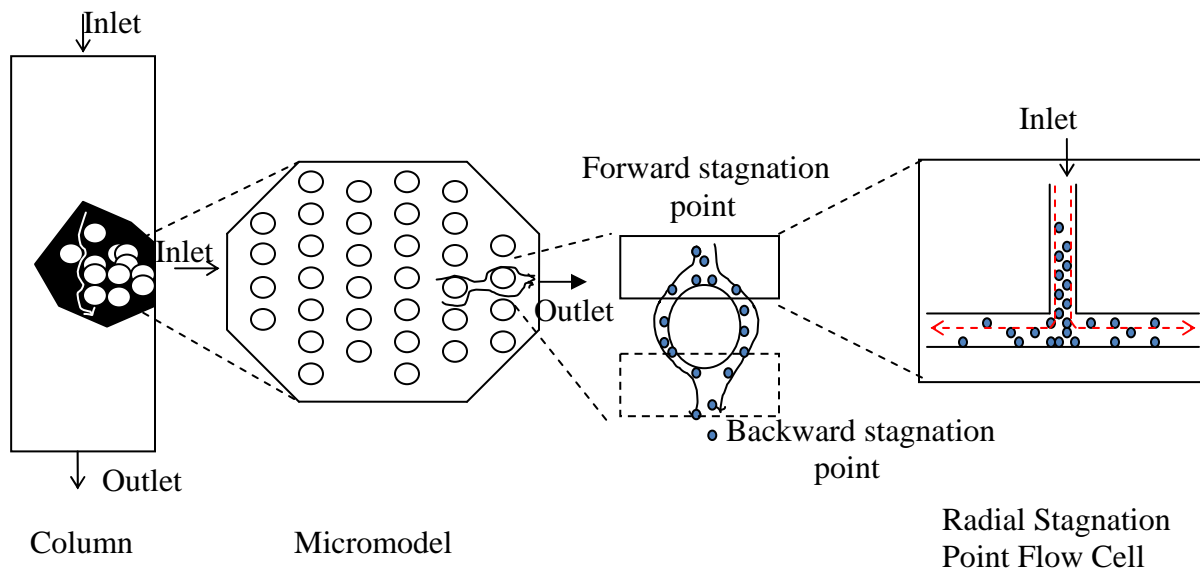


Figure 1 Radial Stagnation Point Flow Cell and Micromodel used in this study

2. Methodology.

Task 1 Characterize *C. parvum* oocyst wall properties

1) Purification of *C. parvum* oocysts. *C. parvum* oocysts (viable, 4-5 μ m in diameter) were purified from the feces of male Holstein calves (IACUC protocol # 04070). The purified oocysts

were centrifuged and washed with Tris-ethylenediamine-tetraacetic acid (Tris-EDTA: 50 mM Tris, 10 mM EDTA) and stored at 4 °C in a solution of 50% Hanks' balanced salt solution (HBSS, GIBCO, Grand Island, New York) and 50% antibiotic-antimycotic solution (0.6% penicillin, 1% streptomycin, 0.0025% amphotericin, and 0.85% NaCl in sterile water).

2) Modification of *C. parvum* oocyst wall. We treated *C. parvum* oocysts with various digestive enzymes, including proteinase K (a broad-spectrum serine protease) and mixed glycosidases (capable of removing carbohydrate residues from proteins). Deposition kinetics of untreated and treated oocysts on quartz surface were also determined to study the effects of oocyst surface macromolecules on oocyst deposition.

3) Characterization of *C. parvum* oocyst wall macromolecules composition and conformation. The peptides released by proteinase K and carbohydrates hydrolyzed by mixed glycosidases were respectively analyzed with liquid chromatography/nano-electrospray ionization tandem mass spectrometry (LC-MS/MS) and phenol-sulfuric acid assay to determine the composition of *C. parvum* oocyst wall surface macromolecules. Surface potential and polarity of the untreated and proteinases treated *C. parvum* oocysts revealed information about the conformation of oocyst wall surface macromolecules.

Task 2 Determine the attachment mechanisms of *C. parvum* oocysts on inorganic and organic surfaces at the microscopic level

A radial stagnation point flow (RSPF) cell was used to determine the attachment efficiency of untreated and proteinase K treated *C. parvum* oocysts on quartz surfaces in the presence of monovalent cations. In addition, the deposition of untreated oocysts on quartz or natural organic matter in the presence of divalent cations was studied in RSPF cell. As seen in Figure 1, RSPF is used to mimic the forward stagnation point of irregular soil grains. With RSPF, it is possible to control the hydrodynamic conditions and conduct real time observation of *C. parvum* oocyst deposition on inorganic and organic surfaces under a microscope.

Task 3 Simulate the transport of *C. parvum* oocysts in the subsurface environment with micromodel and column setup

The micromodel (surface material: SiO₂), as shown in Figure 1, was designed to conduct direct and real time observation of *C. parvum* oocysts traveling along the granular particles. The collectors were etched onto a Si wafer and then the surface was oxidized to form SiO₂. electrolyte solutions containing oocysts were pumped into the micromodel and directly observed under microscope.

3. Principal Findings and Significance.

Each task of the proposed research provided knowledge on deposition and transport of pathogens in the natural environment.

- 1) For task 1, we characterized the composition and conformation of *Cryptosporidium parvum* oocyst wall surface macromolecules and studied their effect on interactions between *C. parvum* oocyst and quartz surface. The results illustrated that *C. parvum* oocyst wall is covered by a fluffy layer of glycoprotein.
- 2) For task 2, we studied the deposition of *C. parvum* oocysts on quartz and natural organic matter surface in the presence of divalent cations and deposition kinetics of untreated and

proteinase K treated *C. parvum* oocysts on quartz surface in the presence of monovalent cations. The results indicated that the fluffy layer on *C. parvum* oocysts wall leads to weaker van der Waals interaction and stronger steric repulsion. This fluffy layer makes oocysts more mobile in the subsurface environment. In addition, carboxyl groups of the fluffy layer on *C. parvum* oocysts wall and natural organic matter surface leads to specific interaction of Ca^{2+} with carboxyl groups and enhanced deposition of oocysts on SRNOM surfaces and decreases the mobility of oocysts in the subsurface environment.

- 3) A microscopic method for direct and real time observation of oocyst transport and distribution in a micromodel that simulates porous media is being developed.

4. Notable Achievements.

- 1) For task 1, we, for the first time, reported contact angles measured for oocysts and based on these data estimated the Hamaker constant between oocysts and quartz surface. The Hamaker constant is essential to calculate van der Waals interaction between those two surfaces.
- 2) For task 2, we found that proteinase K treated *C. parvum* oocysts significantly decreased compared to that of untreated oocysts. This observation indicated that the fluffy layer on *C. parvum* oocysts wall leads to weaker van der Waals interaction and stronger steric repulsion. Inductive coupled plasma (ICP) was employed to measure the free divalent cation concentration in solutions containing oocysts. ICP data showed more Ca^{2+} bound to oocyst surface than Mg^{2+} . Moreover, proteinase K treatment of oocysts led to a significant decrease in deposition rate due to less binding of Ca^{2+} to the surface of the treated oocysts as shown by the ICP data. The deposition and ICP results suggested that inner-sphere complexation of Ca^{2+} with carboxylate groups on both SRNOM and oocyst surfaces enhanced deposition of oocysts on a SRNOM surface.
- 3) For task 3, as of May 2010, we are developing a microscopic method to directly measure single-collector attachment efficiency of *C. parvum* oocysts.

5. Students Supported with Funding.

Ms. Yuanyuan Liu, Department of Civil and Environmental Engineering, Engineering School, University of Illinois at Urbana-Champaign. She is a PhD candidate and is expected to graduate in 2012.

6. Publications and Presentations.

Janjaroen, D.; **Liu, Y.**; Kuhlenschmidt, M. S.; Kuhlenschmidt, T. B.; Nguyen, T. H. Role of Divalent Cations on Deposition of *Cryptosporidium parvum* Oocysts on Natural Organic Matter Surfaces. *Environmental Science & Technology* 2010, in press, DOI: 10.1021/es9038566.

Liu, Y.; Kuhlenschmidt, M. S.; Kuhlenschmidt, T. B.; Nguyen, T. H. Characterization of *Cryptosporidium parvum* Oocyst Wall Macromolecules and Adhesion Kinetics of Oocysts on Quartz Surface. *Biomacromolecules* 2010, Submitted.

Liu, Y.; Kuhlenschmidt, M. S.; Kuhlenschmidt, T. B.; Nguyen, T. H. "Direct measurement of single-collector attachment efficiency of *Cryptosporidium parvum* oocysts: Method development", *239th ACS National Meeting & Exposition*, Mar. 2010

Liu, Y.; Kuhlenschmidt, M. S.; Kuhlenschmidt, T. B.; Yau P. M.; Nguyen T. H. “Role of *C. parvum* Oocysts Wall Macromolecules on Deposition Kinetics of Oocysts on Quartz Surface”
The Association of Environmental Engineering and Science Professors (AEESP), July, 2009

Information Transfer Program Introduction

None.

Universities Council on Water Resources Conference

Basic Information

Title:	Universities Council on Water Resources Conference
Project Number:	2008IL199B
Start Date:	2/1/2008
End Date:	9/1/2009
Funding Source:	104B
Congressional District:	15 th
Research Category:	Not Applicable
Focus Category:	Education, None, None
Descriptors:	
Principal Investigators:	Lisa Merrifield, Jennifer Fackler, Richard E. Warner

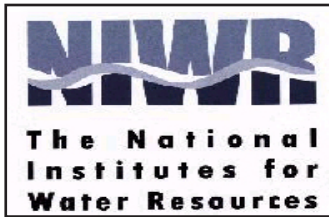
Publications

There are no publications.

IWRC was selected to host the 2009 Universities Council on Water Resources/National Institute for Water Resources conference in Chicago, Illinois. In 2008, IWRC staff began planning the conference. IWRC achievements have included finding an affordable and appropriately equipped venue, planning tours and activities beyond the meeting, soliciting a call for papers and organizing technical sessions, outfitting a steering committee to select and invite plenary speakers and guide overall conference planning, securing conference co-sponsors, and designing, maintaining and updating the conference web site and registration forms.

Following are excerpts from preliminary program.

Urban Water Management: Issues and Opportunities



SPECIAL EVENTS

See page 13 for details.

TUESDAY July 7

REGISTRATION 7:00AM-4:00PM

Cont. Breakfast 7:30AM-8:00AM

PLENARY SESSION 1
8:00AM-10:00AM

Welcome and Keynote Speakers

- Michael Sturtevant
- David Naftzger

Break 10:00AM-10:30AM

TECHNICAL SESSIONS 1
10:30AM-12:00PM

- 2 Stormwater Management I
- 3 Human Impacts on Water Resources
- 4 Agricultural Methods, Practices and Policy

Lunch on Your Own 12:00PM-1:30PM

TECHNICAL SESSIONS 2
1:30PM-3:00PM

- 5 Stormwater Management II
- 6 Ecosystem Impacts and Management Practices
- 7 International Water Supply Policies and Practices

Break 3:00PM-3:30PM

TECHNICAL SESSIONS 3
3:30PM-5:00PM

- 8 Balancing Urban Water Supply and Demand
- 9 Stormwater Management Models
- 10 Pharmaceuticals and Personal Care Product Impact on Water Quality

WELCOME RECEPTION AND POSTER SESSION

Marriot Lower Foyer

6:00PM-8:00PM
TUESDAY JULY 7

MONDAY July 6

Stickney Water Reclamation
District 1:30PM-4:00PM

Metropolitan WRD Cruise
4:00PM-7:00PM

Registration
4:00PM-7:00PM

TUESDAY July 7

Welcome Reception
and Poster Session

6:00PM-8:00PM

WEDNESDAY July 8

UCOWR Awards & Banquet

Marriott Ballroom

Cash Bar 6:30PM

Banquet 7:00PM-9:00PM

THURSDAY July 9

Racine Pumping Station

1:30PM-3:30PM



2009 Conference at a Glance

<p>WEDNESDAY July 8 REGISTRATION 7:30AM-4:00PM</p>	<p>THURSDAY July 9 REGISTRATION 7:30AM-9:00AM</p>	<p>2009 UCOWR AWARD WINNERS</p>		
<p>Cont. Breakfast 7:30AM-8:00AM PLENARY SESSION 2 8:00AM-10:00AM</p>		<p>Cont. Breakfast 7:30AM-8:00AM TECHNICAL SESSIONS 6 8:30AM-10:00AM</p>		
<p>Keynote Speakers - Mary Ann Dickinson - Ed Archuleta - Alice Miller Keyes</p>	<p>20 Dissertation Winners & Other Research 21 Water Supply Planning and Policy in Illinois 22 International Water Resource Problems</p>		<p>Warren A. Hall Medal <i>Gerald E. Galloway</i> <i>Univeristy of Maryland</i></p>	
<p>Break 10:00AM-10:30AM TECHNICAL SESSIONS 4 10:30AM-12:00PM</p>		<p>Break 10:00AM-10:30AM TECHNICAL SESSIONS 7 10:30AM-12:00PM</p>		
<p>13 Streamflow and Urban Water Management 14 Planning for Water Sustainability 15 Impacts of Organic and Inorganic Contaminants on Water Quality</p>	<p>23 Water Quality Monitoring, Modeling and Management 24 Approaches to Stormwater Management 25 Methods for Augmenting Water Supply</p>		<p>Friends of UCOWR <i>Gretchen Rupp and M. J. Nehasil</i> <i>Montana Water Center</i> <i>Ronald D. Lacewell and Michele Zinn</i> <i>Texas A & M University</i></p>	
<p>Lunch on Your Own 12:00PM-1:30PM TECHNICAL SESSIONS 5 1:30PM-3:00PM</p>		<p>END OF TECHNICAL PROGRAM</p>		
<p>16 Monitoring Water Quality and Quantity 17 Water Policy: Planning, Implementation and Management 18 Groundwater Conservation and Management</p>	<p>TECHNICAL TOURS</p>		<p>Ph.D. Dissertation Natural Science and Engineering <i>To be announced</i></p>	
<p>Break 3:00PM-3:30PM PLENARY SESSION 3 3:30PM-5:00PM</p>		<p>Racine Pumping Station</p>		
<p>Keynote Speakers - Jim Heaney - David Douglas</p>	<p>1:30PM-3:30PM</p>		<p>Ph.D. Dissertation Water Policy and Socioeconomics <i>To be announced</i></p>	
<p>UCOWR BANQUET AND AWARDS CEREMONY</p>				<p>Education and Public Service <i>Alliance for Water Efficiency</i> <i>Illinois-Indiana Sea Grant</i></p>
<p>Marriott Ballroom CASH BAR 6:30PM BANQUET 7:00PM-9:00PM WEDNESDAY JULY 8</p>		<p>2009 UCOWR AWARD WINNERS</p>		

Welcome

Urban Water Management: Issues and Opportunities is the theme of the 2009 UCOWR/NIWR Annual Conference in exciting downtown Chicago. With the term “infrastructure” in the news and on everyone’s minds, are we entering a time of renewal of our aging drinking water, waste water, and storm water systems? Will we, community by community, meet the urban water challenges of the 21st Century? This important conference will include presentations on these topics as well as others as critical as pharmaceuticals in our drinking water and the water resource demands of “green” energy sources such as biofuels.

I would like to invite you to join us in downtown Chicago at the Marriott Courtyard hotel for an exciting and professionally rewarding conference – as well as our reception, annual awards banquet, technical, and recreational tours in the urban heart of the Midwest.

Jay Lund
President, Universities Council on Water Resources



CONFERENCE COMMITTEE

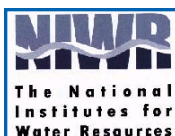
DICK WARNER, UNIVERSITY OF ILLINOIS URBANA-CHAMPAIGN, CHAIR
MARTIN JAFFE, UNIVERSITY OF ILLINOIS-CHICAGO
TIM LOFTUS, CHICAGO METROPOLITAN AGENCY FOR PLANNING
JAY R. LUND, UNIVERSITY OF CALIFORNIA-DAVIS
ARI MICHELSEN, TEXAS AGRILIFE RESEARCH CENTER



CHRISTOPHER LANT, SIUC, UCOWR EXECUTIVE DIRECTOR
ROSIE GARD, SIUC, UCOWR CONFERENCE COORDINATOR
LISA MERRIFIELD, UIUC, LOCAL CONFERENCE COORDINATOR
FARHAT JAHAN CHOWDHURY, SIUC, PUBLICATIONS DESIGNER
STANLEY MUBAKO, SIUC, PUBLICATIONS DESIGNER



UNIVERSITIES COUNCIL ON WATER RESOURCES (UCOWR) is an organization of universities, non-academic institutions, and international affiliates leading in water resources education, research, and public service. UCOWR institutional members and delegates are at the forefront of water resources related research and education. In addition to our annual national conference, UCOWR publishes *The Journal of Contemporary Water Research and Education*. If you would like to join UCOWR, please visit our website at: www.ucowr.siu.edu or call (618) 536-7571.



NATIONAL INSTITUTES FOR WATER RESOURCES (NIWR) are the 54 university-based centers that were established by the federal Water Resources Research Act. They are charged with arranging for research that addresses water problems or expands understanding of water and water-related phenomena, aiding the entry of new professionals into the water resources fields, helping to train future water scientists and engineers, and transmitting research results to water managers and the public.

Plenary Speakers

Plenary Session 1Chicago and the Great Lakes Compact.....Tuesday July 7, 8:30-10:00am



Michael Sturtevant has worked in the water industry for 28 years and has been with the Department of Water Management for the past 15 years. He presently is head of the Planning and Operations Section within the Bureau of Engineering Services. Prior to that he worked as a project manager for the engineering consulting firm, Pitometer Associates for 13 years where he conducted numerous hydraulic engineering studies with various utilities throughout the country. Michael graduated from Michigan Technological University with a Bachelor of Science in Civil Engineering. He is a member of AWWA and ASCE is a registered professional engineer in Illinois.

David Naftzger serves as Executive Director of the Council of Great Lakes Governors. David facilitated the negotiation of the Great Lakes-St. Lawrence River Basin Water Resources Compact. He also oversees six foreign trade offices promoting State exports; the regional biomass energy program; and, the regional tourism partnership. Previously, David was the National Conference of State Legislatures' director for agriculture and international trade in Washington, D.C. David earned a Master's degree in Government from the London School of Economics. He holds a Bachelor's degree in Political Science from DePauw University and studied at the University of Freiburg, Germany.



Plenary Session 2.....Drought Preparedness across the Country.....Wednesday July 8, 8:00-10:00am



Mary Ann Dickinson is the founder and Executive Director of the Alliance for Water Efficiency, a non-profit organization dedicated to promoting the efficient and sustainable use of water in the United States and Canada. Based in Chicago, the Alliance works with water utilities, water conservation professionals in business and industry, planners, regulators, and consumers. Mary Ann has over 35 years of experience in water resources and water efficiency. She is a fellow at the Water Resources Center at the University of California at Santa Cruz, a Trustee and past Chair of the American Water Works Association National Water Conservation Division, and has presented numerous papers on water conservation in Spain, France, Australia, Korea, Jordan, Israel, Italy, Chile, China, Romania, Canada, and all across the United States.

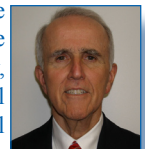
Edmund G. "Ed" Archuleta has been manager of the El Paso Water Utilities Public Service Board since January 1989. A registered Professional Engineer in Texas, New Mexico, and Iowa, he is responsible for all aspects of water, wastewater, reclaimed water service, and storm water to the greater El Paso metropolitan area. He is an American Academy of Environmental Engineers Diplomat. He was appointed in June 2006 by President George W. Bush to the National Infrastructure Advisory Council. In 2008, he was appointed a Committee Member of the National Research Council, National Academy of Science and Engineering to assess water reuse as an alternative for meeting future water supply needs.



Alice Miller Keyes has served as advisor on water conservation and efficiency to the EPD Director since 2004. She helped develop Georgia's comprehensive statewide water management plan and coordinated the development of Georgia's Water Conservation Implementation Plan. Alice has 15 years of experience in water policy and planning. She serves as a charter board member of the Alliance for Water Efficiency and the Georgia WaterWise Council. She has a Master's in Conservation Ecology/Sustainable Development from University of Georgia and a Bachelor's in Biology from University of Southern Mississippi.

Plenary Session 3...Cutting Edge Research and Water for the Poor...Wednesday July 8, 3:30-5:00pm

Jim Heaney received his PhD in environmental and water resources engineering from Northwestern University. Currently, he is Professor and Chair of the Department of Environmental Engineering Sciences at the University of Florida. He specializes in the application of decision support systems to developing more sustainable urban water infrastructure systems including water supply, wastewater, and stormwater. Dr. Heaney is a former President of UCOWR. He has served on numerous committees of the National Academy of Sciences dealing with water and environmental issues. He is a Diplomat of the American Academy of Environmental Engineers and a Diplomat of the American Academy of Water Resources Engineers.



David Douglas



WELCOME AND INTRODUCTIONS

8:00am - 8:30 am

Jay R. Lund, UCOWR President, University of California, Davis

Upton Hatch, NIWR President, North Carolina WRRI; North Carolina State University

PLENARY 1 Chicago and the Great Lakes Compact

8:30 am – 10:00 am

Michael Sturtevant, Head, Planning and Operations, Bureau of Engineering Services, Chicago

David Naftzger, Executive Director, Council of Great Lakes Governors

----- *BREAK 10:00 am – 10:30 am* -----

CONCURRENT TECHNICAL SESSIONS

10:30 am – 12:00 pm

Session 2 Stormwater Management I

Survey of Stormwater BMP Maintenance Practices. *John S. Gulliver*, University of Minnesota, Minneapolis, MN; Andrew J. Erickson, _____; Joo-Hyon Kang, _____; Peter T. Weiss, _____; C. Bruce Wilson _____.

Improving Urban Stormwater Quality: Applying Fundamental Principles. *Allen P. Davis*, University of Maryland, College Park, MD; Robert G. Traver, Villanova University, Villanova, PA; William F. Hunt, North Carolina State University, Raleigh, NC.

Watershed Retrofit and Management Evaluation for Urban Stormwater Management Systems in North Carolina. *William F. Hunt*, Upton Hatch, Olha Sydorovych, and Kathy DeBusk, North Carolina State University, Raleigh, NC.

Application of the Analytic Hierarchy Process to Stormwater BMP Selection. *Kevin Young*, Tamim Younos, Randy Dymond, and David Kibler, Virginia Tech, Blacksburg, VA.

Session 3 Human Impacts on Water Resources

Human Interferences to Streamflow Dynamics: A Case Study of Urban Watersheds. *Dingbao Wang*, Ximing Cai, and Murugesu Sivapalan, University of Illinois, Urbana, IL.

Calibrating Hydrologic/Hydraulic Models of an Urban Watershed - Upper Salt Creek. *Wade Moore*, MWH Americas, Chicago, IL.

Comparative Modeling of Streamflow Response in an Intensively Managed Urban Watershed. *Hongyi Li*, Jiing-Yun You, Ximing Cai, and Murugesu Sivapalan, University of Illinois, Urbana, IL.

Integrating Science into Policy: The Use of Climate Information in Municipal Water Resources Management. *Christine Kirchhoff*, University of Michigan, Ann Arbor, MI.

Session 4 Agricultural Methods, Practices, and Policy

Rate Analyses for Irrigation Districts in South Texas. *Allen Sturdivant* and Edward Rister, Texas A&M University, Weslaco, TX; Ronald D. Lacewell, Texas A&M Agriculture Office of Federal Relations, College Station, TX.

Water Resource Requirements of Corn-Based Ethanol. *Stanley Mubako* and Christopher Lant, Southern Illinois University Carbondale, Carbondale, IL.

Water Policy in the Southern High Plains: A Farm Level Analysis. *Justin Weinheimer* and Phillip Johnson, Texas Tech University, Lubbock, TX.

Agency Problems in Irrigation Water Transfer: Who Works for What? *John Wiener*, University of Colorado, Boulder, CO.

----- *LUNCH ON YOUR OWN 12:00 pm – 1:30 pm* -----

CONCURRENT TECHNICAL SESSIONS

1:30 pm – 3:00 pm

Session 5 Stormwater Management II

Infiltration Pond Design Considerations for Cold Weather Conditions. *Steve S. Nelson*, Michael E. Barber, and David R. Yonge, Washington State University, Pullman, WA.

Implementing Watershed-Based Green Infrastructure for Stormwater Management: Case Study in Blacksburg, Virginia. *Meredith Warren* and Tamim Younos, Virginia Tech, Blacksburg, VA.

Integration of Education, Scholarship, and Service through Stormwater Management. *Robert G. Traver*, Andrea Welker, and Bridget Wadzuk, Villanova University, Villanova, PA.

Stormwater Management for a Record Rainstorm in Chicago. *Stanley A. Changnon*, University of Illinois, Champaign, IL.

Session 6 Ecosystem Impacts and Management Practices

Toward Identifying Optimal Best Management Practices for Watershed Management of Water Quality. *M. Edward Rister*, Ronald D. Lacewell, Taesoo Lee, Raghavan Srinivasan, Balaji Narasimhan, Texas Agrilife Research, College Station, TX; Allen W. Sturdivant, Texas AgriLife Research and Extension Center, Weslaco, TX; Clint Wolfe, David Waidler, Texas AgriLife Research and Extension Urban Solutions Center, Dallas, TX; Darrel Andrew, Mark Ernst, Jennifer Owens, Tarrant Regional Water District, Fort Worth, TX.

Impacts of Road Salt on Water Resources in the Chicago Region. *Walton Kelly*, Samuel V. Panno and Keith C. Hackley, Illinois State Geological Survey, Champaign, IL.

McDowell Grove Dam Removal. *Kristine Meyer*, Christopher B. Burke Engineering West, Ltd., St. Charles, IL.

Determining Optimal Reservoir Release for Both Water Supply and Ecosystem Restoration. *Yi-Chen Yang* and Ximing Cai, University of Illinois, Urbana, IL.

Session 7 International Water Supply Policies and Practices

Sustainable Control of Water-Related Infectious Diseases: A Review and Proposal for Interdisciplinary Health-Based Systems Research. *Stuart Batterman*, Jonathan Bulkley, Joseph Eisenberg, Rebecca Hardin, Margaret Kruk, Elisha Renne, Maria Lemos, Bhramar Mukherjee, Anna M. Michalak, Howard Stein, Cristy Watkins, and Mark Wilson, University of Michigan, Ann Arbor, MI.

Water in Pune District, Maharashtra State, India: Economic, Environmental and Management Issues. *Subhash Bhagwat*, University of Illinois Institute for Natural Resources Sustainability, Champaign, IL.

Community Mobilization Models for Safe Water Supply: Experiences from the Developing World. *Farhat Chowdhury*, Southern Illinois University Carbondale, Carbondale, IL.

Ergonomic Aspects in the Bottled Water Delivery in Ciudad Juarez, Chihuahua, Mexico. *Marana-Teresa Escobedo*, Salvador Noriega Morales, and Jorge A. Salas Plata Mendoza, Universidad Autonoma de Ciudad Juarez, Ciudad Juarez, Chihuahua, Mexico.

----- **BREAK 3:00 pm – 3:30 pm** -----

CONCURRENT TECHNICAL SESSIONS

3:30 pm – 5:00 pm

Session 8 Balancing Urban Water Supply and Demand

Urban Water Demand Analysis of Five Border Cities of Northwestern Mexico. *Josue Medellin-Azuara*, University of California-Davis, Davis, CA.

Water Sustainability: Results of the Army Installation Water Study. *Natalie Myers*, US Army Corps of Engineers, ERDC/CERL, Champaign, IL.

Water Demand and Supply Outlook for the Greater Chicago Area. *Benedykt Dziegielewski*, Southern Illinois University Carbondale, Carbondale, IL.

Revealing the Trade-Offs When Aiming for a Quantitative Balance in England's River Rother. *John Joyce*, IPA Energy + Water Economics, London, England; Benoit Grandmougin, ACTEON, Colmar, France.

Governor's Conference on the Illinois River

Basic Information

Title:	Governor's Conference on the Illinois River
Project Number:	2008IL200B
Start Date:	2/1/2008
End Date:	11/1/2009
Funding Source:	104B
Congressional District:	15th
Research Category:	Not Applicable
Focus Category:	Education, None, None
Descriptors:	
Principal Investigators:	Lisa Merrifield, Jennifer Fackler

Publications

There are no publications.

The Governor's Conference on the Illinois River is held biennially in odd years. The next conference will be held on October 20-22, 2009 in Peoria, Illinois. IWRC cosponsors the conference by serving on the planning committee and designing the abstract book and conference proceedings. This year, IWRC staff member, Lisa Merrifield, has also participated in the Local Action subcommittee and secured a speaker on implementing pharmaceutical take back programs. Merrifield will also be moderating a session on local action success stories with respect to the Illinois River.

The Governor's Conference on the Illinois River web site is available at <http://www.conferences.uiuc.edu/ilriver/>.

Transferring Water Resources Information to the People of Illinois

Basic Information

Title:	Transferring Water Resources Information to the People of Illinois
Project Number:	2009IL174B
Start Date:	3/1/2009
End Date:	2/28/2010
Funding Source:	104B
Congressional District:	15
Research Category:	Not Applicable
Focus Category:	None, None, None
Descriptors:	None
Principal Investigators:	Lisa Merrifield

Publication

1. Merrifield, Lisa, ed., 2009, Proceedings for the Governor's Conference on the Illinois River. Champaign, Illinois.

Newsletter

Once per year, usually in late summer, the Illinois Water Resources Center publishes a newsletter detailing our research and outreach activities over the previous year. The newsletter is distributed to over 700 people on our mailing list and is made available on our website.

Governor's Conference on the Illinois River

The Governor's Conference on the Illinois River took place this past year—2009—on October 20-22, in Peoria, Illinois. IWRC co-sponsored the conference by serving on the planning committee and designing the abstract book and conference proceedings. This year, IWRC staff member, Lisa Merrifield, participated in the Local Action subcommittee and secured a speaker on implementing pharmaceutical take back programs. Merrifield also moderated a session on local action success stories with respect to the Illinois River.

A web site on the 2009 conference is available at <http://www.conferences.uiuc.edu/ilriver/>. The next Governor's Conference on the Illinois River will be held in 2011.

Water Conference 2010

The statewide Illinois Water conference is held biennially in even years. It is lead by IWRC staff members with the intention of sharing the latest research findings related to Illinois water resources. The theme for the October 2010 conference will be water quality, quantity, and sustainability. Sessions will include water supply sustainability; climate change; Asian carp research, management and outreach; and an update on the Illinois water supply plan.

Web Site

The IWRC web site has long been an access point for people seeking information about water resources in Illinois. We continue to maintain the IWRC research and special report library as well as provide access to upcoming events and our newsletter via the web site.

Illinois Steward Magazine

IWRC has provided support for Illinois Steward Magazine, which has the following mission: "*The Illinois Steward* is an award-winning nature magazine that is grounded in the "land ethic" of Aldo Leopold. *The Illinois Steward* features articles about stewardship, conservation, preservation, and restoration of natural areas in Illinois. Article topics include native plants, wildlife, natural areas in Illinois, nature photography, and Illinois' historical past."

The magazine is published quarterly and regularly includes articles on water resources issues because of IWRC support.

2009 University Council on Water Resources Conference

IWRC hosted the 2009 Universities Council on Water Resources/National Institute for Water Resources conference in Chicago, Illinois. IWRC staff coordinated the conference and organized

the call for papers and session architecture. The theme capitalized on the urban location and brought people from Chicago and around the country to talk about urban water issues.

UCOWR President, Jay Lund wrote about the conference, “Urban Water Management: Issues and Opportunities is the theme of the 2009 UCOWR/NIWR Annual Conference in exciting downtown Chicago. With the term “infrastructure” in the news and on everyone’s minds, are we entering a time of renewal of our aging drinking water, waste water, and storm water systems? Will we, community by community, meet the urban water challenges of the 21st Century? This important conference will include presentations on these topics—as well as others as critical as pharmaceuticals in our drinking water and the water resource demands of ‘green’ energy sources, such as biofuels.”

Approximately 250 people from around the country attended.

USGS Summer Intern Program

None.

Student Support					
Category	Section 104 Base Grant	Section 104 NCGP Award	NIWR-USGS Internship	Supplemental Awards	Total
Undergraduate	2	0	0	0	2
Masters	1	0	0	0	1
Ph.D.	1	0	0	0	1
Post-Doc.	0	0	0	0	0
Total	4	0	0	0	4

Notable Awards and Achievements